NASA/TM-2013-217512

The Ice, Cloud and land Elevation Satellite (ICESat): Summary Mission Timeline and Performance Relative to Pre-Launch Mission Success Criteria

Charles E. Webb, H. Jay Zwally, and Waleed Abdalati

National Aeronautics and
Space Administration

Goddard Space Flight Center
Greenbelt, Maryland 20771

June 2013

NASA STI Program ... in Profile

Since its founding, NASA has been dedicated to the advancement of aeronautics and space science. The NASA scientific and technical information (STI) program plays a key part in helping NASA maintain this important role.

The NASA STI program operates under the auspices of the Agency Chief Information Officer. It collects, organizes, provides for archiving, and disseminates NASA's STI. The NASA STI program provides access to the NASA Aeronautics and Space Database and its public interface, the NASA Technical Report Server, thus providing one of the largest collections of aeronautical and space science STI in the world. Results are published in both non-NASA channels and by NASA in the NASA STI Report Series, which includes the following report types:

- TECHNICAL PUBLICATION. Reports of completed research or a major significant phase of research that present the results of NASA Programs and include extensive data or theoretical analysis. Includes compilations of significant scientific and technical data and information deemed to be of continuing reference value. NASA counterpart of peer-reviewed formal professional papers but has less stringent limitations on manuscript length and extent of graphic presentations.
- TECHNICAL MEMORANDUM. Scientific and technical findings that are preliminary or of specialized interest, e.g., quick release reports, working papers, and bibliographies that contain minimal annotation. Does not contain extensive analysis.
- CONTRACTOR REPORT. Scientific and technical findings by NASA-sponsored contractors and grantees.
- CONFERENCE PUBLICATION. Collected papers from scientific and technical conferences, symposia, seminars, or other meetings sponsored or co-sponsored by NASA.
- SPECIAL PUBLICATION. Scientific, technical, or historical information from NASA programs, projects, and missions, often concerned with subjects having substantial public interest.
- TECHNICAL TRANSLATION. English-language translations of foreign scientific and technical material pertinent to NASA's mission.

Specialized services also include organizing and publishing research results, distributing specialized research announcements and feeds, providing help desk and personal search support, and enabling data exchange services. For more information about the NASA STI program, see the following:

- Access the NASA STI program home page at http://www.sti.nasa.gov
- E-mail your question via the Internet to help@sti.nasa.gov
- Fax your question to the NASA STI Help Desk at 443-757-5803
- Phone the NASA STI Help Desk at 443-757-5802
- Write to:

  NASA STI Help Desk
  NASA Center for AeroSpace Information
  7115 Standard Drive
  Hanover, MD 21076-1320

NASA/TM-2013-217512

The Ice, Cloud and land Elevation Satellite (ICESat): Summary Mission Timeline and Performance Relative to Pre-Launch Mission Success Criteria

Charles E. Webb
Goddard Space Flight Center, Greenbelt, MD
H. Jay Zwally
Goddard Space Flight Center, Greenbelt, MD
Waleed Abdalati
NASA Headquarters, Washington, D.C.

National Aeronautics and
Space Administration

Goddard Space Flight Center
Greenbelt, Maryland 20771

June 2013

Level of Review: This material has been technically reviewed by technical management

Available from:
NASA Center for AeroSpace Information
7115 Standard Drive
Hanover, MD 21076-1320

National Technical Information Service
5285 Port Royal Road
Springfield, VA 22161 Price Code: A17

The Ice, Cloud and land Elevation Satellite (ICESat): Summary Mission Timeline and Performance Relative to Pre-Launch Mission Success Criteria

Charles E. Webb, Ph.D.
Principal Scientist, SGT Inc.
Goddard Space Flight Center
Cryospheric Sciences Laboratory

H. Jay Zwally, Ph.D.
ICESat Project Scientist
Goddard Space Flight Center
Cryospheric Sciences Laboratory

Waleed Abdalati, Ph.D.
Chief Scientist
NASA Headquarters

Executive Summary

On June 22, 2010, NASA initiated the decommissioning of the Ice, Cloud and land Elevation Satellite (ICESat) by powering down its on-board instrument, the Geoscience Laser Altimeter System (GLAS). This document reviews the scientific achievements of the mission, particularly with respect to the Mission Success Criteria (MSC) established prior to launch, which stated that ICESat would produce:

(1) A significant improvement in the measurement of the ice sheet surface elevation changes over previous radar altimetry estimates to $dh/dt < 2$ cm/year (1σ value);

(2) Calibrated profiles of global land and ocean surface elevations, especially at high latitudes where there is currently no detailed comprehensive data;

(3) Calibrated profiles of ice sheet surface elevation to better than 25 cm accuracy at the ground location of each laser pulse, to serve as a basis for comparisons to future elevation observations.

Although technical problems were encountered with the lasers on orbit, the GLAS instrument team worked closely with the ICESat science team to develop a modified operations plan. **As a result, ICESat has met or exceeded each of the requirements established to define the mission as a success.**

First, elevation change results from Greenland show that $\sigma_{dh/dt}$ is ~1 cm/yr for most of the ice sheet, and that larger errors observed along the margins have been significantly reduced relative to previous radar remote-sensing missions. Second, although the pre-launch changes to the MSC increased the emphasis on cryospheric science, calibrated elevation profiles have been routinely produced over ocean and land surfaces, throughout the mission, at latitudes up to $\pm 86°$. Third, elevation differences from intra-campaign crossovers in Antarctica have a standard deviation of 25 cm or less for surfaces with slopes less than 2°, which encompasses the vast majority of the ice sheet.

ICESat data has also been used to make significant scientific contributions outside the areas defined by the MSC. In particular, it played a critical role in the discovery of new subglacial lakes in Antarctica, enhancing our understanding of water transfer beneath the surface. ICESat also contributed important information about sea-ice freeboard and thickness at a time of record-low extent in the Arctic Ocean. Finally, despite technical problems with the green channel, remarkably detailed profiles of the planetary boundary layer and atmospheric aerosols were obtained for the first time.

1. Introduction

The Ice, Cloud and land Elevation Satellite (ICESat) mission was conceived, primarily, to quantify the spatial and temporal variations in the topography of the Greenland and Antarctic ice sheets. It carried on board the Geoscience Laser Altimeter System (GLAS), which measured the round-trip travel time of a laser pulse emitted from the satellite to the surface of the Earth and back. Each range derived from these measurements was combined with precise, concurrent orbit and pointing information to determine the location of the laser spot centroid on the Earth. By developing a time series of precise topographic maps for each ice sheet, changes in their surface elevations can be used to infer their mass balances.

The following section summarizes the Mission Success Criteria (MSC) established for the ICESat mission. Section 3 provides an overview of ICESat mission operations, from launch through decommissioning, and discusses the on-orbit technical challenges faced by the instrument and science teams. Section 4 assesses the overall performance of the ICESat observatory with respect to the MSC, and Section 5 reviews additional scientific contributions made using data collected during the mission. Section 6 describes the ICESat data products and where they have been archived.

2. Mission Success Criteria

The Level-1 requirements in the EOS Program Plan (February 2001) established an initial set of MSC for the ICESat mission. Prior to launch, however, the Single Photon Counting Modules – the detectors for the atmospheric green channel – were determined to be unreliable, but they were declared to be non-essential for the success of the mission. As a result, the MSC were modified, and documented in a separate memorandum, dated December 2002 (see Appendix A). The official Level-1 requirements were not updated at that time, nor at any time since. The revised MSC defined success as "an improvement by a significant factor over our current knowledge of ice sheet elevation variability and mass balance." Specifically, they stated that ICESat would produce:

(1) A significant improvement in the measurement of the ice sheet surface elevation changes over previous radar altimetry estimates to $dh/dt < 2$ cm/year (1σ value);

(2) Calibrated profiles of global land and ocean surface elevations, especially at high latitudes where there is currently no detailed comprehensive data;

(3) Calibrated profiles of ice sheet surface elevation to better than 25 cm accuracy at the ground location of each laser pulse, to serve as a basis for comparisons to future elevation observations.

3. Mission Summary

The ICESat mission began with a launch on January 12, 2003, from Vandenberg Air Force Base, on a Boeing Delta-II rocket. The first of the three lasers in the on-board GLAS instrument was commanded to begin firing on February 20. The initial returns showed strong and well-behaved waveforms, yielding high-quality surface and cloud elevation measurements. After only two weeks, however, the laser energy began to decline at a much faster rate than expected, with some indications suggesting problems in the laser pump diodes. This decline continued until March 29, when Laser 1 ceased firing after 36 days of on-orbit operation.

The Independent GLAS Anomaly Review Board (IGARB) was assembled to: (1) determine the cause of the premature failure of Laser 1; (2) assess the likelihood of similar failures for Lasers 2 and 3; and (3) recommend steps to prolong the on-orbit lifetimes of the two remaining lasers in support of the overall mission objectives. In its report, the board concluded that an excess of indium solder, applied during the manufacture of the laser diode arrays, contributed to the failure of Laser 1. The interaction of this solder with gold conducting wires led to the formation of gold-indide compounds, which gradually corroded the wires. A second contributing factor in the failure was the development of a shunt current in a diode array bar, forcing the redistribution of current among the gold wires. This accelerated gold-indide formation and increased thermal stresses, causing wire fatigue, and eventually, a short to ground, which fused the bond wires open.

Based on its analysis of the Laser 1 failure, the IGARB recommended that Laser 2 be operated at a lower temperature, to slow the growth of the gold-indide compounds. Furthermore, in anticipation of similarly shortened lifetimes for the two remaining lasers, the mission operations plan was revised to balance spatial and temporal coverage requirements in support of the scientific objectives. The planned 183-day repeat cycle was replaced with a 91-day repeat cycle, but a decision was made to operate GLAS only during a 33-day near-repeat subcycle of this new orbit, three times per year: Winter (February/March), Spring (May/June) and Fall (September/October).

With this revised operational scenario in place, Laser 2 began firing on September 25, 2003, while in the 8-day repeat cycle of the calibration orbit. As with Laser 1, the initial returns provided high-quality surface and cloud elevation measurements. The satellite transitioned to the 91-day repeat cycle on October 4, and GLAS was scheduled to continue operating for one complete 33-day subcycle. Further analysis of the early science data, however, suggested a misalignment of the laser beam within the telescope field-of-view. Prior to launch, it had been determined that this alignment was sensitive to the temperature of the GLAS optical bench, and that, as a result, a minimum temperature of 16.2°C should be maintained. Nonetheless, due to difficulties with the control of the component

loop heat pipe that regulated this temperature, the ICESat project decided to begin Laser 2 operations with a bench temperature of 14.2°C.

After the misalignment was revealed, a command to raise the temperature of the component loop heat pipe was uploaded to the satellite, in an attempt to steer the laser beam more into the telescope field of view. Unfortunately, because the memory configuration of the ground command test bed did not map directly to the configuration on board the satellite, this command erroneously raised the temperature of the *laser* loop heat pipe. The error was recognized within a single orbit pass, and corrected within another. Subsequent commands successfully raised the temperature of the component loop heat pipe, and the beam alignment noticeably improved. The ICESat project then extended the period of operations for Laser 2 by two weeks, to allow for the collection of a complete 33-day data set following the alignment correction.

Shortly after the unintended thermal spike to the laser, the transmit energy began to decline more rapidly. A newly constituted GLAS Anomaly Review Board (GARB), consisting of internal GSFC laser experts, concluded that it was likely the result of a photo-darkening process occurring at and near the GLAS frequency doubler, which converts a portion of the laser-output near-infrared (1064 nm) beam to a green (532 nm) wavelength, for use in the atmospheric measurements. The board observed that the electrical power required to heat the doubler decreased as the laser energy declined, suggesting that the laser light passing through the doubler crystal was being increasingly absorbed. They concluded that this was likely due to trace levels of hydrocarbons, outgassed from adhesives used in the laser, interacting with the 532-nm photons. The command error that led to the increase in the laser temperature probably accelerated this process.

This operations period, designated the L2a campaign, came to an abrupt end on November 19, when the on-board computer was reset after a new basetime was uploaded, triggering the satellite to enter a sun-acquisition, safe-hold mode. Given the proximity to the planned end date for the campaign, two days later, and the initial uncertainty surrounding the cause of the computer reset, the ICESat project decided to delay any restart of Laser 2 until the following Spring opportunity in 2004.

Lasting for a total of 55 days, the L2a campaign consumed approximately one-third of the laser's energy for altimetry. As the Spring 2004 opportunity approached, the ICESat project proposed significantly lowering the laser temperature, from 27°C to 16°C. Initially, the GARB opposed this because it would involve operating the laser at a temperature outside the nominal limits, and for which there was little test data. This issue was not resolved in time for the Spring opportunity, and the L2b campaign began on February 17, 2004. Shortly after, during an around-the-world calibration scan, the satellite entered a sun-acquisition, safe-hold mode, when an unfavorable Sun geometry caused limits

in the flight software to be violated. The satellite was reoriented, and science data collection resumed within 12 hours. The laser energy output steadily declined until March 5, when the transmit gain was increased. The transmit energy stabilized for several days, before resuming a gradual decline, and the campaign concluded on March 21.

After additional deliberation, the GARB unanimously recommended lowering the laser temperature to 16°C, and the necessary commands were uploaded early in the L2c campaign, which began on May 18, 2004. Once this temperature change was implemented, the rate of laser energy decline slowed significantly, leaving approximately 5 mJ available for altimetry by the end of the Summer 2004 opportunity. By this point, Laser 2 had operated on orbit for nearly three times as long as Laser 1, a reflection of the lessons learned by the instrument team, and establishing a solid basis for Laser 3 operations. As a result, a decision was made to switch to Laser 3 for future campaigns, and to return to Laser 2 only when the former's energy had been depleted.

On October 3, 2004, Laser 3 was commanded to begin firing at the start of the Fall opportunity. Table 1 summarizes all of the campaigns conducted with this laser. The 532-nm (green) energy was significantly lower than expected, and the GARB later concluded that this was likely due to a mechanical shift of the doubler crystal, caused by shrinkage of the polymer used in its mount. The near-infrared energy for altimetry, however, declined at a much slower rate than for either of the other lasers. This has been attributed to the lower operating temperature of the laser, a longer outgassing time, and lower green energy, all of which contribute to reduced levels of photo-darkening. Laser 3 ceased firing on October 19, 2008, after a total of 354 days on on-orbit operation.

2004	L3a	03 Oct – 08 Nov
2005	L3b	17 Feb – 24 Mar
	L3c	20 May – 23 Jun
	L3d	21 Oct – 24 Nov
2006	L3e	22 Feb – 28 Mar
	L3f	24 May – 26 Jun
	L3g	25 Oct – 27 Nov
2007	L3h	12 Mar – 14 Apr
	L3i	02 Oct – 05 Nov
2008	L3j	17 Feb – 21 Mar
	L3k	04 Oct – 19 Oct

Table 1. ICESat Laser 3 Campaigns

After several failed attempts to restart Laser 3, the ICESat project decided to return to Laser 2. The orbit was adjusted to shift the satellite back to the reference ground tracks that were covered at the end of the L3k campaign, and Laser 2 was restarted on November 25, 2008. After falling below 3 mJ, the laser transmit energy was boosted by increasing the laser temperature on December 9, in accordance with earlier GARB recommendations. This produced a much larger-than-expected jump in the output energy, to more than 8 mJ. At the conclusion of the L2d campaign, on December 17, the laser retained nearly 5 mJ, about what it had at the end of the L2c campaign, more than four years earlier.

With the advent of the Spring 2009 opportunity, Laser 2 was restarted, on March 9. During the L2e campaign, an impressive number of returns were obtained at unprecedented low-energy levels. The laser transmit energy was allowed to decline to nearly 1 mJ. Another, although smaller, increase in the laser temperature again boosted the output energy, which remained stable at 2 mJ until the campaign concluded on April 11. On September 30, the L2f campaign commenced. The transmit laser energy declined gradually, until the laser stopped firing on October 11. After several failed attempts to restart Laser 2, restarts of the other two lasers were attempted, but none succeeded. Decommissioning of the ICESat spacecraft began with powering off the GLAS instrument on June 22, 2010.

4. On-Orbit Performance

Despite the challenges posed by reduced laser lifetimes and limited operational periods, the ICESat mission has demonstrated a remarkable advance in satellite remote sensing of the Earth. The GLAS instrument team worked closely with the science team to understand the technical problems encountered with the lasers. Together, they developed a modified operations plan that extended the lifetimes of the remaining lasers well beyond what was expected after the failure of Laser 1.

This section discusses the results obtained in pursuit of the primary scientific objectives of the mission, as expressed by the revised MSC listed in Section 2. For each criterion, ICESat has met or exceeded the requirement established to define the mission as a success.

Criterion 1

Produce a significant improvement in the measurement of the ice sheet surface elevation changes over previous radar altimetry estimates to $dh/dt < 2$ cm/year (1σ).

Prior to the launch of ICESat, Zwally et al. (2002) outlined a procedure for assessing the error in the derived dh/dt estimates using crossover analysis. At

points where ascending and descending tracks cross, the elevations interpolated from the two profiles are differenced and divided by the time between the observations, yielding *dh/dt*. Averaging these crossover *dh/dt* values over a large enough area (e.g., a typical 100 km x 100 km drainage basin) reduces the error of the spatially averaged *dh/dt* to less than 2 cm/year.

After the failure of Laser 1, the adoption of the seasonal campaign strategy shifted the emphasis for *dh/dt* recovery from crossovers to repeat-track analysis. The science data, however, revealed that the elevation profiles were typically offset horizontally from the targeted reference track, due to pointing control errors, with offsets varying between 56 and 111 meters (RMS) for different campaigns (Webb et al., 2010).

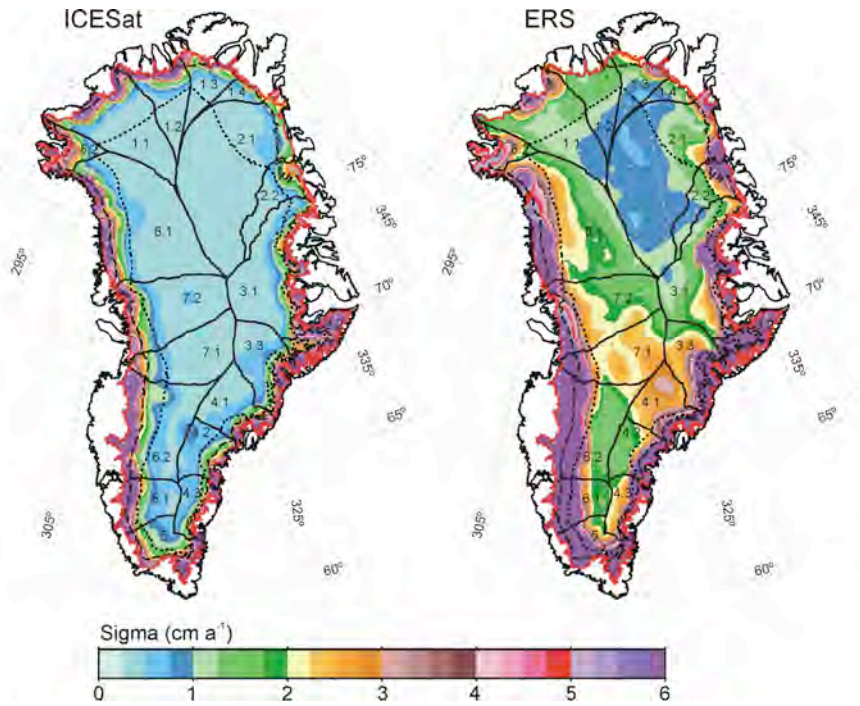

Figure 1. [Left] Map of $\sigma_{<dH/dt>}$ for ICESat (2003-2007), computed from cell-averaged <dH/dt> solutions at individual reference points (Zwally et al., submitted). [Right] Map of $\sigma_{dH/dt}$ for ERS (1992-2002), computed from time-series analysis of crossover differences (Zwally et al., 2005)

Figure 1 illustrates the 1σ errors associated with the *dh/dt* estimates obtained for Greenland, from ICESat data (2003-2007) and from ERS data (1992-2002). The ICESat results show a clear and significant improvement in accuracy, particularly in the interior of the ice sheet. In this region, which constitutes the vast majority of its area, 1σ errors are below 1 cm/year. Furthermore, along the

margins of the ice sheets, where the rates of elevation change are much higher, the bands of larger errors have been dramatically narrowed.

ICESat has measured elevation change in Greenland with an accuracy of < 1 cm/year over the majority of the ice sheet

Criterion 2

Produce calibrated profiles of global land and ocean surface elevations, especially at high latitudes where there is currently no detailed comprehensive data.

The change to the ICESat MSC, in December 2002, increased the emphasis on cryosphere measurements for the mission. Despite this, and the limitations posed by the spatial and temporal coverage, the ICESat data products constitute a substantial, consistently referenced land elevation data set, with unprecedented accuracy and quantified measurement errors. With support from the NASA Earth Surface and Interior program, ICESat data is being used to build a global geodetic ground control point (GCP) database to improve existing digital elevation models (DEMs), such as those from the Shuttle Radar Topography Mission (SRTM) and the Advanced Spaceborne Thermal Emission and Reflection Radiometer (ASTER). Each ICESat waveform provides a unique sampling of the elevations within a particular laser footprint (Harding and Carabajal, 2005). In forested areas, this has enabled the determination of the height of the SRTM elevations, measured at the radar phase center, within the vegetation canopy.

Figure 2 shows an example of this application for Australia, where differences between the ICESat elevation profiles and the SRTM DEM revealed 5-meter amplitude, undulating errors in the latter, over hundreds of kilometers (Carabajal et al., 2010). The continental-scale coverage afforded by ICESat can be used to remove these long-wavelength errors from the DEM. Figure 2 also highlights the consistency in the mean elevation differences, across various ICESat campaigns, suggesting very stable performance of the GLAS instrument.

In addition, the United States Geological Survey has led a collaborative effort to assess the accuracy of five ASTER Global DEM (GDEM) tiles, using various sources of ground control, including ICESat-derived geodetic GCPs (Carabajal et al., 2009). Figure 3 illustrates this work, and similar evaluations of an improved version of the ASTER GDEM will be made before it is released. Furthermore, the inclusion of ICESat data during the production of DEMs from other sensors, such as Interferometric Synthetic Aperture Radar (InSAR) enhances the quality of regional models, enabling better process modeling and interpretation (Atwood et al., 2007).

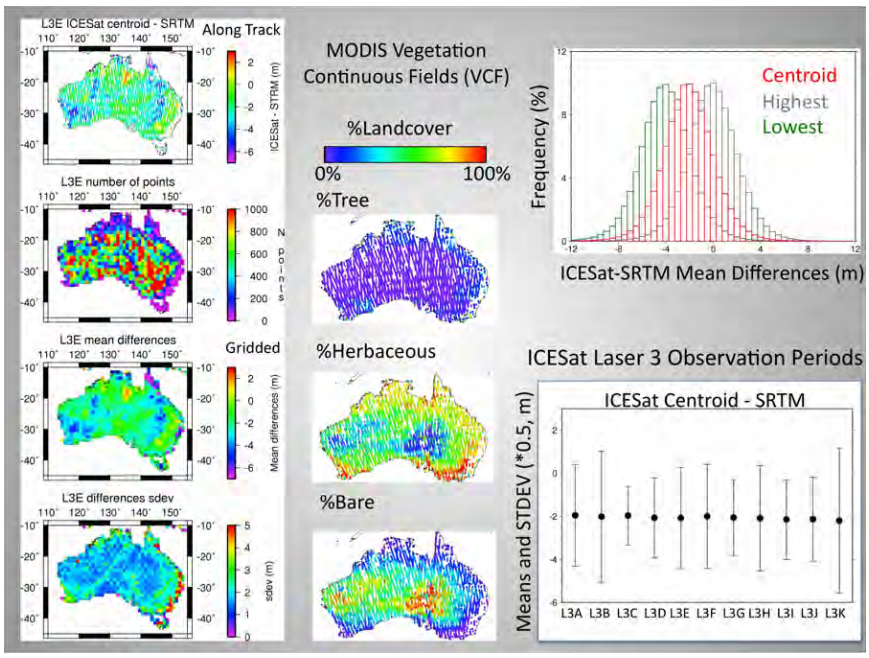

Figure 2. [Left] Mean ICESat centroid – SRTM differences for the L3e observation period. [Center] MODIS land-cover classification. [Right] Histograms of elevation differences for highest, centroid and lowest ICESat elevations (top) and means and standard deviations for centroid elevation differences during Laser 3 campaigns (bottom). (Carabajal et al., 2010)

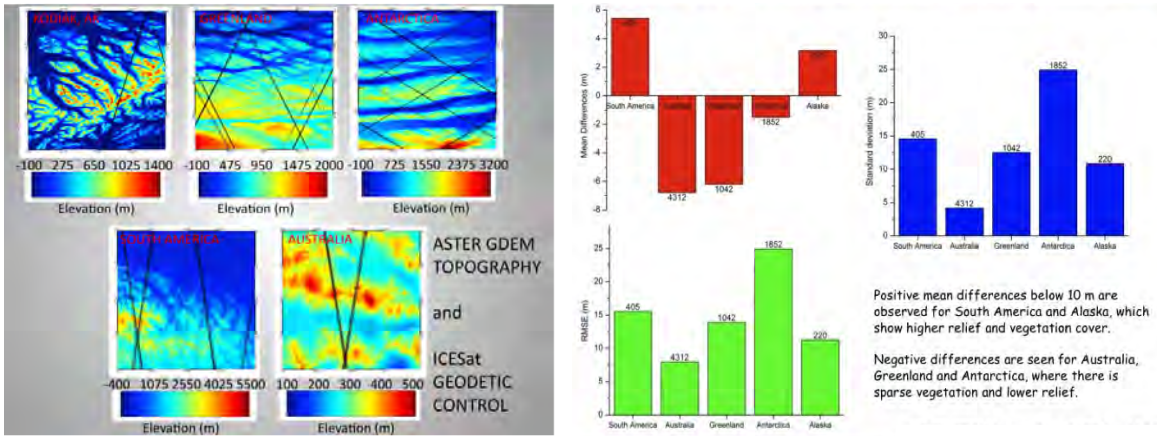

Figure 3. Evaluation of ASTER DEM tiles, using ICESat altimetry: [Left] ASTER topography with ICESat elevation profiles (black) as geodetic GCPs. [Right] Summary statistics for elevation differences for each tile. (Carabajal et al., 2009)

One of the most important, and challenging, land applications for ICESat data concerns the characterization and monitoring of vegetative cover. The Center for Ecological Applications of Lidar (CEAL) at Colorado State University is investigating the use of lidar remote sensing to study three-dimensional ecosystem spatial structure. They have used ICESat data, in conjunction with multi-spectral Moderate Resolution Imaging Spectroradiometer (MODIS) data, to create a global map of forest canopy height, which is shown in Figure 4.

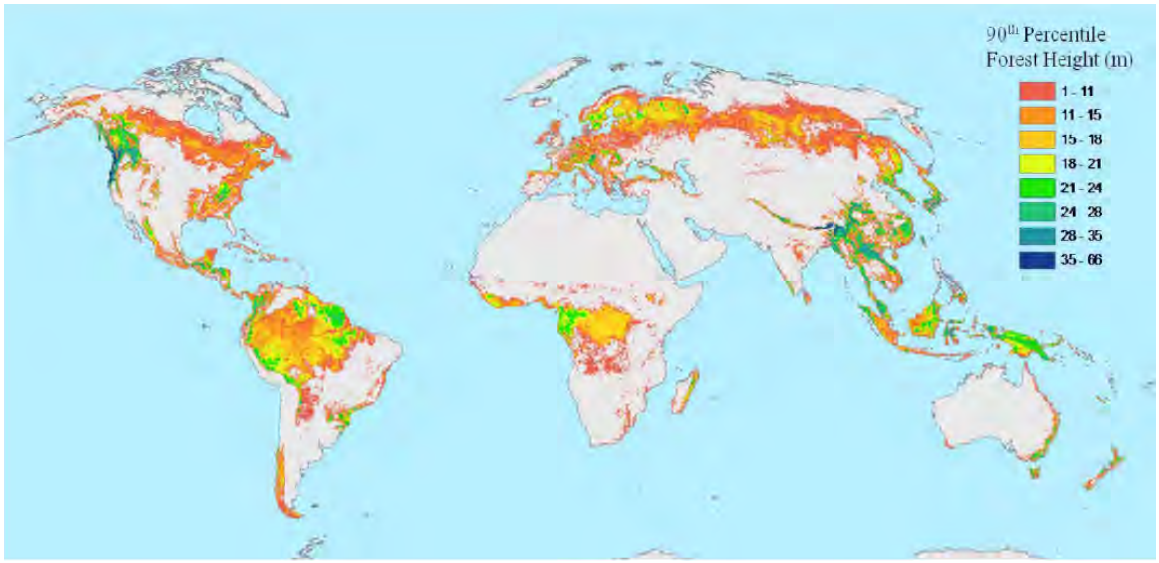

Figure 4. Global forest height map. Heights are the 90th percentile of GLAS height observations within a MODIS patch (Lefsky, 2010)

Global ocean surface profiles have been produced routinely with ICESat data. Spatial coverage of the oceans extends to ±86°, well beyond the ±66° latitude limits of traditional, radar-based oceanographic missions, such as TOPEX/Poseidon and Jason 1/2. Urban and Schutz (2005) compared global ocean elevations from ICESat, collected during the L2a campaign, to concurrent measurements made by TOPEX/Poseidon. Figure 5 illustrates a 10-cm bias between the two satellites, which they found by computing the sea-surface anomaly (SSA, measured elevation minus mean sea surface) for each. Furthermore, they noted that, because of its inherently higher resolution, ICESat "measures small-scale ocean variability caused by waves, wind effects and swell." Nonetheless, after removing this bias, the agreement between the ocean states observed by ICESat and TOPEX/Posedion (Figures 5a and 5b) is pronounced. Rather than being constant, however, this bias was subsequently found to vary with each ICESat campaign, suggesting a possible link to laser energy levels. The analysis of ocean data continues to play an important role in assessing residual inter-campaign biases, which have also been observed over ice sheets (Gunter et al., 2009).

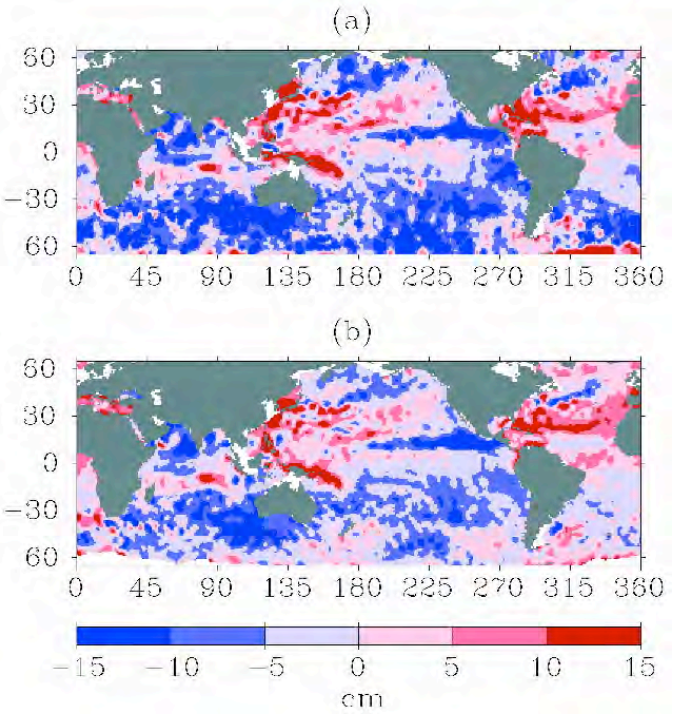

(c)

Figure 5. Global sea surface anomaly (SSA), Sep-Nov 2003: (a) ICESat, -10 cm bias removed; (b) TOPEX; (c) daily averages (Urban and Schutz, 2005)

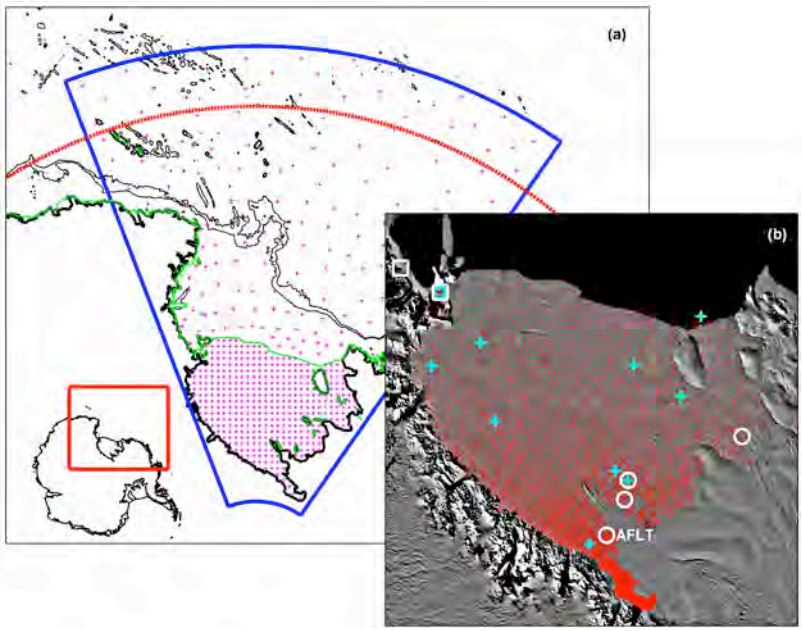

Figure 6. Ross Ice Shelf, Antarctica: (a) blue line outlines model domain, red line delimits southern limit of TOPEX/Poseidon orbit at 66°S, and green line delineates ice front from MODIS Mosaic of Antarctica (MOA); (b) red dots mark ICESat crossovers included in the study, and additional symbols mark validation data sets, including gravimeter records (+), GPS receivers (o), and tide gauges (□). (Padman et al., 2008)

The expanded latitude coverage afforded by ICESat, relative to TOPEX/Poseidon, for example, has allowed for significant improvements to be made to ocean tide models in the polar regions. Notably, Padman et al. (2008) introduced ICESat elevation measurements from the Ross Ice Shelf to improve existing models for ocean tides near Antarctica. They validated their inverse solution using independent *in situ* data sets, including GPS receivers deployed on the ice shelf during the austral summers 2003/04 and 2004/05. Figure 6 illustrates the region and data sets included in their analysis.

ICESat has provided high-quality elevation data over oceans and land, increasing coverage significantly in the polar regions

Criterion 3

Produce calibrated profiles of ice sheet surface elevation to better than 25 cm accuracy at the ground location of each laser pulse, to serve as a basis for comparisons to future elevation observations.

Although dual crossovers — in which the two elevation measurements are from different ICESat campaigns — have been used only on a limited basis in the determination of *dh/dt*, intra-campaign crossovers still provide significant insight into elevation accuracy. In this approach, elevations at locations where ascending and descending tracks cross within a single ICESat campaign are compared. The resulting elevation differences are assumed to represent the combined effects of orbit, ranging and pointing errors, along with any short-term elevation change. Figure 7 summarizes the standard deviation of all intra-campaign crossovers in Antarctica for each of eleven ICESat campaigns, as a function of slope. Nearly all of the campaigns yield σ values below 25 cm for slopes less than 2°, which encompasses the majority of the ice sheet. The one campaign that exceeds this goal is L2a, which suffered from high saturation in the return signal. Improvements in the saturation correction are expected to bring these crossover results in line with other campaigns.

ICESat has measured elevations in Antarctica with an accuracy of < 25 cm over the majority of the ice sheet

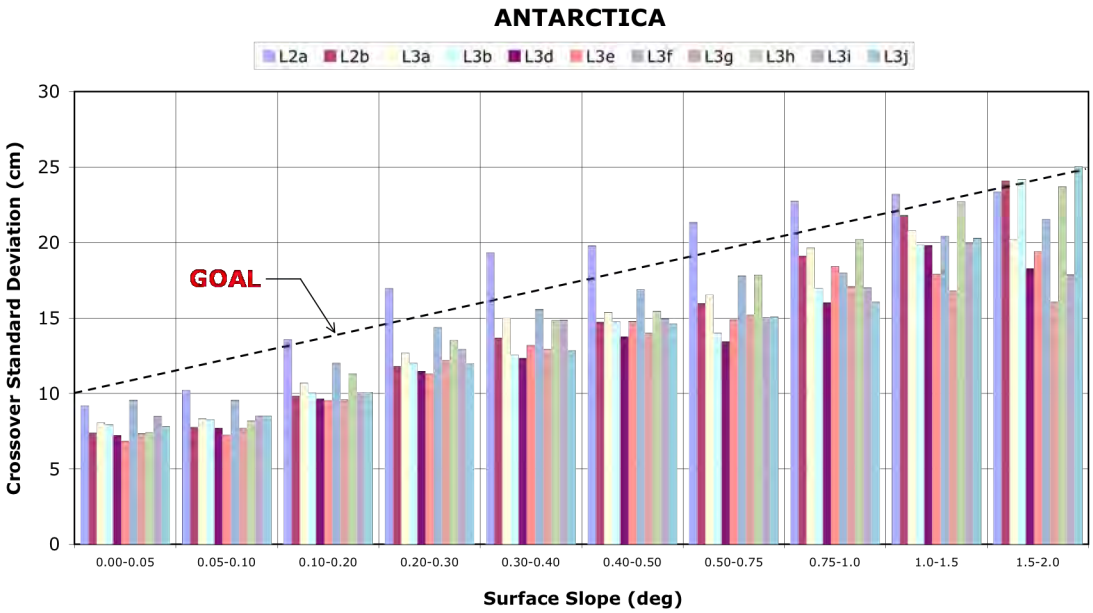

Figure 7. Standard deviations of all Antarctic intra-campaign crossovers versus slope

5. Additional Scientific Contributions

In addition to achieving its primary scientific objectives, ICESat data have been used to make significant contributions outside the areas defined by the MSC. Many of these were published in a 2005 series of three special issues of *Geophysical Research Letters* (Volume 32, Issues 21-23). They have also been detailed in recent ICESat Senior Review proposals (see, for example, GSFC, 2009).

Notably, Fricker et al. (2007) identified specific sites in Antarctica where changes in surface elevation suggested repeated filling and emptying of subglacial lakes, as shown in Figure 8. The volumes of water and their rates of transfer were determined to be much larger than those previously thought possible. Smith et al. (2009) subsequently used ICESat data to produce the first comprehensive survey of subglacial lakes in Antarctica. Figure 9 shows a map of their results.

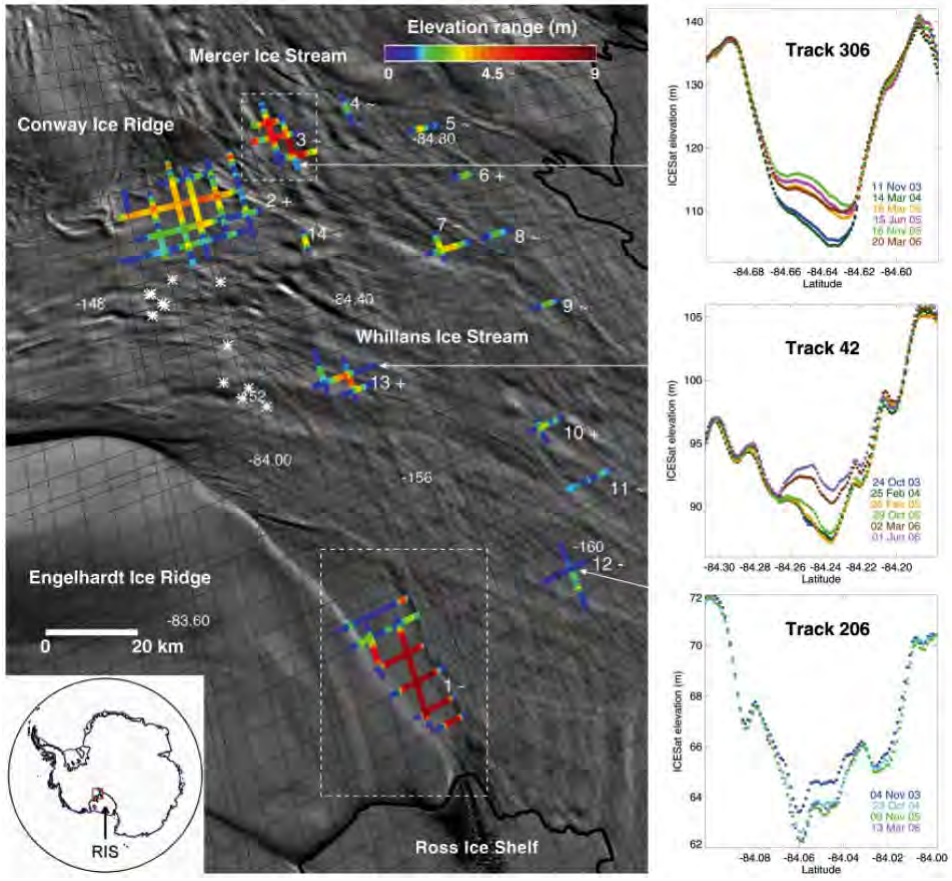

Figure 8. [Left] Locations of elevation change events detected by ICESat on the Whillans and Mercer Ice Streams, with colors indicating the magnitude of the changes. [Right] Repeat ICESat elevation profiles across oscillating (upper), rising (middle) and falling (lower) regions. (Fricker et al., 2007)

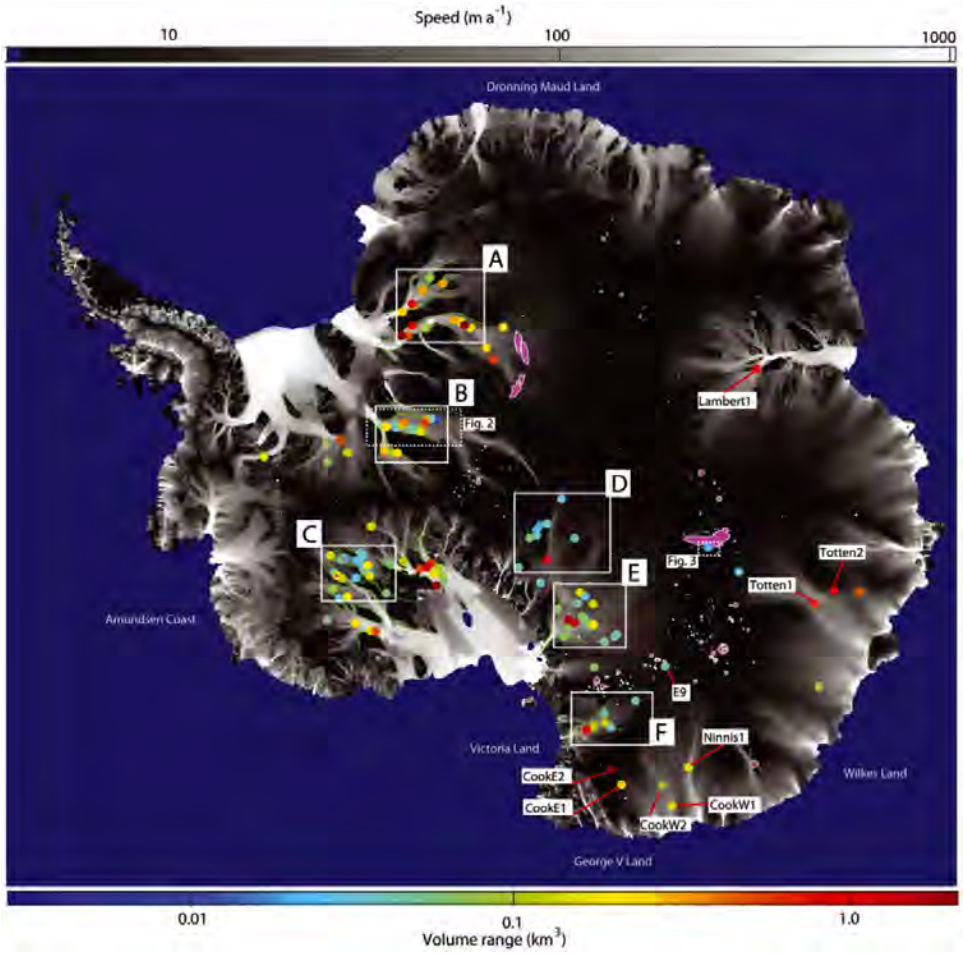

Figure 9. Locations and volume-range estimates for 124 active lakes under the Antarctic ice sheet, with colors indicating volume range. Background shading shows a combination of satellite-radar-derived surface velocities (Joughin et al., 2006) and balance velocities (Bamber et al., 2009). (Smith et al., 2009)

The nature of the ICESat data has also lent itself to the application of techniques from other disciplines. For example, Pritchard et al. (2009) applied triangular irregular networks to ICESat elevations to determine *dh/dt* in both Greenland and Antarctica. Their method allows them to distinguish between dynamically induced elevation changes, and those associated with accumulation or melt. Their results, shown in Figure 10, led them to conclude that "the most profound changes in the ice sheets currently result from glacier dynamics at ocean margins."

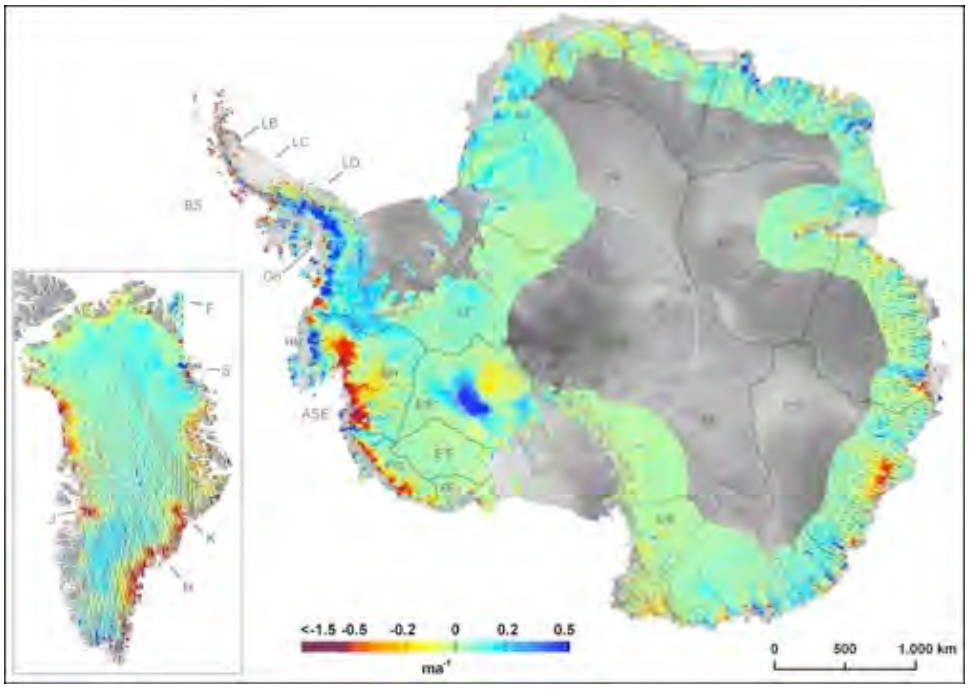

Figure 10. Rates of elevation change for Greenland (left) and Antarctica (right). The white dashed line delineates the southern latitude limit for radar altimetry measurements in Antarctica, and the black lines identify drainage basins (Pritchard et al., 2009)

One of the most important contributions made by ICESat has been its monitoring of sea ice. Farrell et al. (2009) developed a new method for sea-surface height retrieval to compute the first-ever time series of sea ice freeboard in the Arctic Ocean, spanning five years, between 2003 and 2008. They conclude that this trend is "due to thinning of the sea ice pack, rather than changes in snow cover." Figure 11 illustrates the dramatic decline in freeboard that they observed between the start and end of this period.

Kwok and Rothrock (2009) used their ICESat-derived freeboard calculations to generate estimates of sea ice thickness in the Arctic Ocean. They noted a large decline over the same five-year period, from 2003 to 2008. In addition, they examined submarine ice draft data, extending back to 1958, to place the ICESat trends into a broader historical context. Figure 12 shows this overall trend, revealing long-term thinning of Arctic sea ice, beginning in the early 1980s.

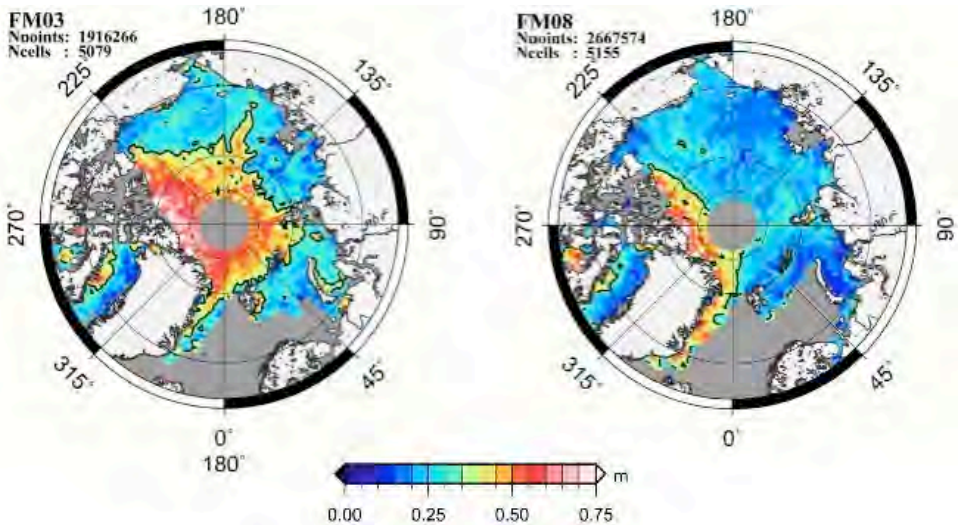

Figure 11. Polar stereographic maps of Arctic sea ice freeboard in February/March 2003 (left) and February/March 2008 (right) (Farrell et al., 2009)

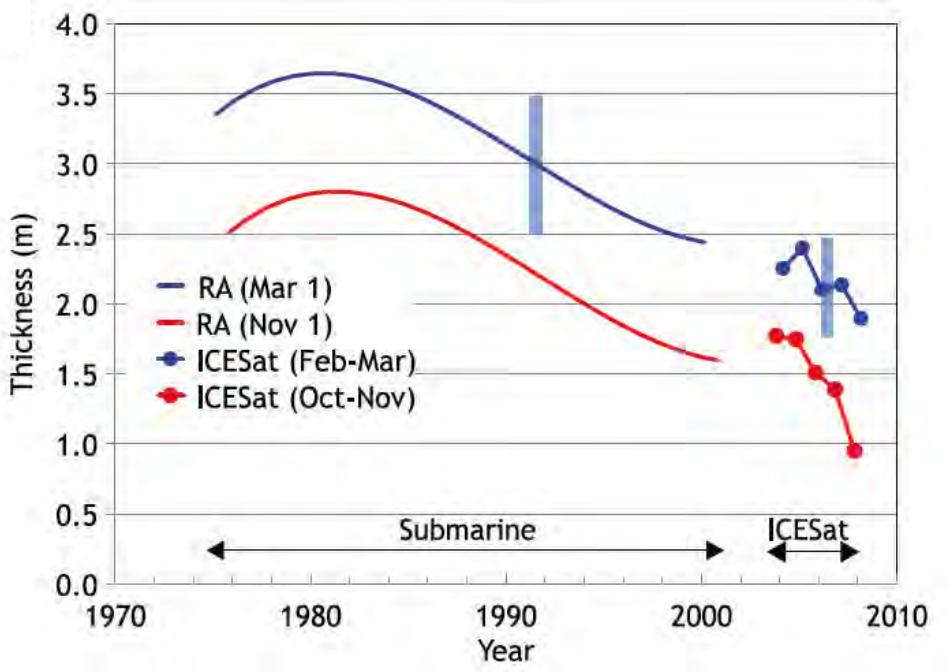

Figure 12. Interannual changes in winter (blue) and summer (red) ice thickness from regression analysis (RA) of submarine data and 10 ICESat campaigns, with error bars shown in blue (Kwok and Rothrock, 2009)

Finally, despite the technical limitations of the 532-nm (green) channel, ICESat has provided remarkable results in atmospheric science. Palm et al. (2005) used GLAS attenuated backscatter data to produce the first-ever global mapping of the depth and structure of the planetary boundary layer (PBL), shown in Figure 13.

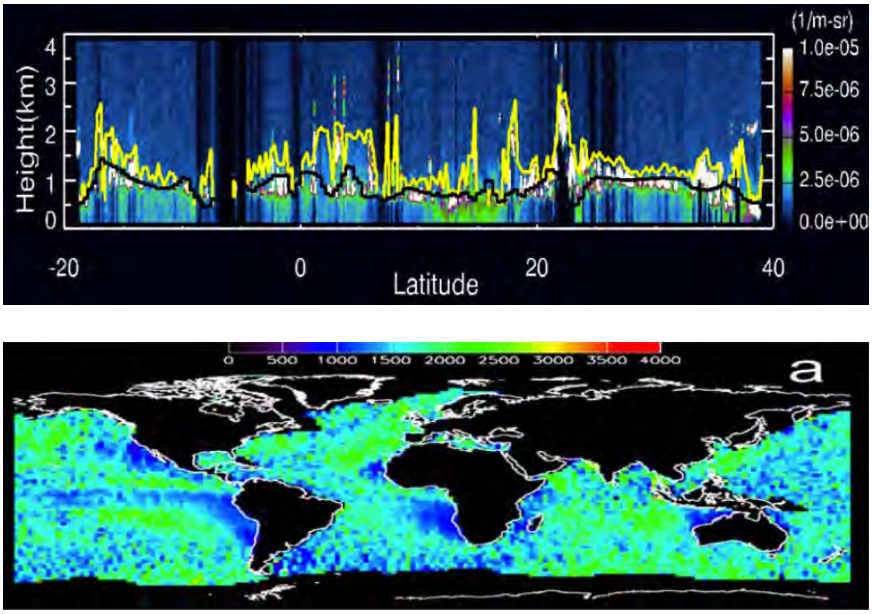

Figure 13. [Top] GLAS attenuated backscatter (yellow) showing the PBL, along with the ECMWF model forecast (black) for Track 52 over the Pacific Ocean on October 1, 2003; [Bottom] Global map of the GLAS-derived PBL for October 2003 (Palm et al., 2005)

Spinhirne et al. (2005) also provided the first global measurements of the true height distribution of aerosol layers in the atmosphere. They found that the 532-nm (green) channel in GLAS provided much better resolution than the 1064-nm (near-infrared) channel. In Figure 14, for example, they noted the finer detail visible in the upper plot, showing aerosols emanating from convective clouds, during a pass over Western Australia.

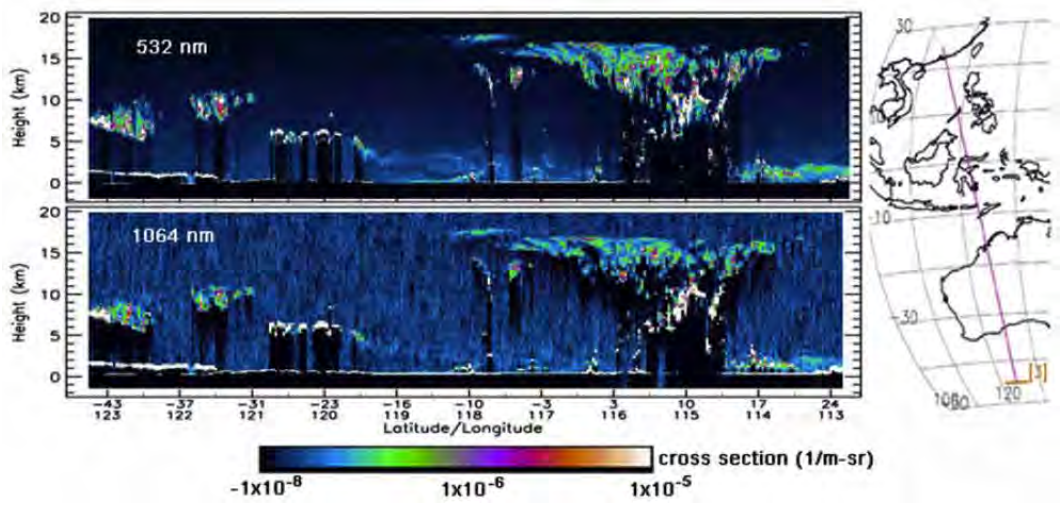

Figure 14. GLAS 532-nm (top) and 1064-nm (bottom) atmospheric data over track shown at right, from Western Australia to southern China (Spinhirne et al., 2005)

6. ICESat Data Products

The National Snow and Ice Data Center (NSIDC), at the University of Colorado at Boulder, archives and distributes 15 ICESat data products. The four Level-1A products, designated GLA01 through GLA04, contain global altimetry, atmosphere, engineering and laser-pointing data, respectively. In addition, global waveform parameters, elevation and backscatter data are available in three Level-1B products: GLA05 through GLA07, respectively. Four of the Level-2 products, GLA08 through GLA11, pertain to atmospheric measurements, providing global data related to the planetary boundary layer, cloud heights, aerosol vertical structure, and optical depth data, respectively. Altimetry data from the Antarctic and Greenland ice sheets, sea ice, land surface, and oceans are available in the final four Level-2 products: GLA12 through GLA15, respectively.

As of this writing, these data products and detailed descriptions of their parameters can be found at: http://nsidc.org/data/icesat/data.html.

7. Acknowledgments

The authors would like to thank the ICESat Science Team, and its leader, Prof. Bob Schutz, of the University of Texas at Austin, for their review of the final manuscript. They would also like to acknowledge the support of the NASA Cryospheric Sciences Program in compiling this assessment.

Bibliography

Abshire, J., X. Sun, and M. Krainak (2005), Laser altimetry using pseudo-noise code modulated fiber lasers and photon counting detectors, *IEEE Quantum Electronics and Laser Science Conference*, 22 May, Baltimore, Maryland, 1991-1993.

Afzal, R., A. Yu, J. Dallas, A. Melak, A. Lukemire, L. Ramos-Izqueirdo, and W. Mamakos (2007), The Geoscience Laser Altimeter System (GLAS) laser transmitter, *IEEE Journal of Selected Topics in Quantum Electronics*, *13* (3), 511-536.

Alsdorf, D., E. Rodriguez, and D. Lettenmaier (2007), Measuring surface water from space, *Reviews of Geophysics*, *45*, RG2002, doi: 10.1029/2006RG000197.

Anselm, B. (2004), Lessons-learned on NASA's EOS/ICESat Mission, *Proceedings of the IEEE Aerospace Conference 2004*, doi:10.1109/ aero.2004.1367594.

Atwood, D., R. Gurtiz, R. Muskett, C. Lingle, J. Sauber, and J. Freymueller (2007), DEM control in Arctic Alaska with ICESat laser altimetry, *IEEE Transactions on Geoscience and Remote Sensing*, *45* (11), 3710-3720.

Baek, S., O. Kwoun, A. Braun, Z. Lu, and C. Shum (2005), Digital elevation model of King Edward VII Peninsula, West Antarctica, from SAR interferometry and ICESat laser altimetry, *IEEE Geoscience and Remote Sensing Letters*, *2* (4), 413-417.

Bamber, J. (2004), Modelling ice sheet dynamics with the aid of satellite-derived topography, in *Spatial Modelling of the Terrestrial Environment*, edited by R. Kelly, N. Drake, and S. Barr, pp. 13-33, John Wiley and Sons, Ltd., West Sussex, England.

Bamber, J. and J. Gomez-Dans (2005), The accuracy of digital elevation models of the Antarctic continent, *Earth and Planetary Science Letters*, *237* (3-4), 516-523.

Bamber, J., J. Gomez-Dans, and J. Griggs (2009), A new 1 km digital elevation model of the Antarctic derived from combined satellite radar and laser data – Part 1: data and methods, *The Cryosphere*, *3*, 101-111.

Beaulieu, A., and D. Clavet (2009), Accuracy assessment of Canadian digital elevation data using ICESat, *Photogrammetric Engineering and Remote Sensing*, *75* (1), 81-86.

Berkoff, T., S. Valencia, E. Welton, and J. Spinhirne (2005), Spatiotemporal path-matching for comparisons between ground-based and satellite lidar measurements, *Óptica Pura y Aplicada*, *39* (1), 109-116.

Berthier E., and T. Toutin (2008), SPOT5-HRS digital elevation models and the monitoring of glacier elevation changes in North-West Canada and South-East Alaska, *Remote Sensing of the Environment*, *112* (5), 2443–2454.

Berthier, S., P. Chazette, J. Pelon, and B. Baum (2008), Comparison of cloud statistics from spaceborne LIDAR systems, *Atmosphere Chemistry and Physics*, *8*, 6965-6977.

Berthier, E., R. Le Bris, L. Mabileau, L. Testut, and F. Rémy (2009), Ice wastage on the Kerguelen Islands (49°S, 69°E) between 1963 and 2006, *Journal of Geophysical Research*, *114*, F03005, doi:10.1029/2008JF001192.

Berthier E., E. Schiefer, G. Clarke, B. Menounos, and F. Remy (2010), Contribution of Alaskan glaciers to sea level rise derived from satellite imagery, *Nature Geoscience*, *3* (2), 92-95, doi:10.1038/ngeo737.

Bhang, K., F. Schwartz, and A. Braun (2007), Verification of the vertical error in C-band SRTM DEM using ICESat and Landsat-7, Otter Tail County, MN, *IEEE Transactions on Geoscience and Remote Sensing*, *45* (1), 36-44.

Bills, B., A. Borsa, and R. Comstock (2007), MISR-based passive optical bathymetry from orbit with few-cm level of accuracy on the Salar De Uyuni, Bolivia, *Remote Sensing of Environment*, *107* (1-2), 240-255.

Bindschadler, R., H. Choi, C. Shuman, and T. Markus (2005), Detecting and measuring new snow accumulation on ice sheets by satellite remote sensing, *Remote Sensing of Environment*, *98* (4), 388-402.

Borsa, A., J.-B. Minster, B. Bills, and H. Fricker (2007), Modeling long-period noise in kinematic GPS applications, *Journal of Geodesy*, *81* (2), 157-170.

Borsa, A., H. Fricker, B. Bills, J.-B. Minster, C. Carabajal, and K. Quinn (2008), Topography of the Salar De Uyuni, Bolivia from kinematic GPS, *Geophysical Journal International*, *172* (1), 31-40.

Boudreau, J., R. Nelson, H. Margolis, A. Beaudoin, L. Guindon, and D. Kimes (2008), Regional aboveground forest biomass using airborne and spaceborne LiDAR in Québec, *Remote Sensing of the Environment*, *112* (10), 3876-3890.

Bourgoin, L., M.-P. Bonnet, J.-M. Martinez, P. Kosuth, G. Cochonneau, P. Moreira-Turcq, J.-L. Guyot, P. Vauchel, N. Filizola, and P. Seyler (2007), Temporal dynamics of water and sediment exchanges between the Curuaí floodplain and the Amazon River, Brazil, *Journal of Hydrology*, *335* (1-2), 140-156.

Braun, A., K. Cheng, B. Csathó, and C. Shum (2004), ICESat laser altimetry in the Great Lakes, *Proceedings of the 60th Annual Meeting of the Institute of Navigation*, Dayton, Ohio, 7-9 June, 409-416.

Braun, A. and G. Fotopoulos (2007), Assessment of SRTM, ICESat, and survey control monument elevations in Canada, *Photogrammetric Engineering and Remote Sensing*, *73* (12), 1333-1342.

Braun, M., A. Humbert, and A. Moll (2009), Changes of Wilkins Ice Shelf over the past 15 years and inferences on its stability, *The Cryosphere,* 3, 41-56.

Brenner, A., J. DiMarzio, and H. Zwally (2007), Precision and accuracy of satellite radar and laser altimeter data over the continental ice sheets, *IEEE Transactions on Geoscience and Remote Sensing*, *45* (2), 321-331.

Carabajal, C. and D. Harding (2005), ICESat validation of SRTM C-band digital elevation models, *Geophysical Research Letters*, *32*, L22S01, doi:10.1029/2005GL 023957.

Carabajal, C. (2006), SRTM C-band and ICESat laser altimetry elevation comparisons as a function of tree cover and relief, *Photogrammetric Engineering and Remote Sensing*, *72* (3), 287-298.

Carabajal, C. and D. Harding (2006), SRTM C-band and ICESat laser altimetry elevation comparisons as a function of tree cover and relief, *Photogrammetric Engineering and Remote Sensing*, *72* (3), 287-298.

Carabajal, C., D. Harding and V. Suchedo (2009), ASTER GDEM validation using ICESat altimetry, contribution to ASTER Global DEM Validation Summary Report, edited by ASTER GDEM Validation Team: METI/ERSDAC, NASA/LPDAAC, USGS/EROS, in cooperation with NGA and others, https://lpdaac.usgs.gov/lpdaac/products/aster_products_table/routine/global_ digital_elevation_model/v1/astgtm.

Carabajal, C., D. Harding and V. Suchedo (2010), ICESat lidar and global digital elevation models: Applications to DESDynI, Paper 4200, IEEE International Geoscience and Remote Sensing Symposium, Honolulu, Hawaii, 25-30 July.

Carter, S., D. Blankenship, D. Young, M. Peters, J. Holt, and M. Siegert (2009), Dynamic distributed drainage implied by the flow evolution of the 1996–1998 Adventure Trench subglacial lake discharge, *Earth and Planetary Science Letters*, *283* (1), 24-37.

Casey, S., A. Dessler, and C. Schumacher (2007), Frequency of tropical precipitating clouds as observed by the Tropical Rainfall Measuring Mission Precipitation Radar and ICESat/Geoscience Laser Altimeter System, *Journal of Geophysical Research 112*, D14215, doi: 10.1029/2007JD008468.

Chen, Q. (2010), Assessment of terrain elevation derived from satellite laser altimetry over mountainous forest areas using airborne lidar data, *ISPRS Journal of Photogrammetry and Remote Sensing*, *65* (1), 111-122.

Chen, Q. (2010), Retrieving canopy height of forests and woodlands over mountainous areas in the Pacific Coast region using satellite laser altimetry, *Remote Sensing of Environment*, doi:10.1016/j.rse.2010.02.016.

Chepfer, H., M. Chiriaco, R. Vautard, and J. Spinhirne (2007), Evaluation of MM5 optically thin clouds over Europe in Fall using ICESat lidar spaceborne observations, *Monthly Weather Review*, *135* (7), 2737-2753.

Chipman, J. (2007), Satellite-based assessment of the dynamics of new lakes in southern Egypt, *International Journal of Remote Sensing*, *28* (19), 4365-4379.

Chunbo, F., L. Jiancheng, W. Dan, C. Yonghai, X. Xinyu, and Z. Xiancai (2005), Applications of ICESat to geoscience research, *Journal of Geodesy and Geodynamics*, *25* (2), 94-97.

Crétaux, J.-F., R. Létolle, and S. Calmant (2009), Investigations on Aral Sea regressions from mirabilite deposits and remote sensing, *Aquatic Geochemistry*, *15* (1-2), 277-291.

Csathó, B., Y. Ahn, T. Yoon, C. van der Veen, S. Vogel, G. Hamilton, D. Morse, B. Smith, and V. Spikes (2005), ICESat measurements reveal complex pattern of elevation changes on Siple Coast ice streams, Antarctica, *Geophysical Research Letters*, *32*, L23S04, doi: 10.1029/2005GL024289.

Dalå N., R. Forsberg, K. Keller, H. Skourup, L. Stenseng, and S. Hvidegaard (2005), Airborne lidar measurements of sea ice north of Greenland and Ellesmere Island 2004, *Technical Report 1/2005*, Danish National Space Center, Copenhagen, Denmark.

Dessler, A., S. Palm, W. Hart, and J. Spinhirne (2006), Tropopause-level thin cirrus coverage revealed by ICESat/Geoscience Laser Altimeter System, *Journal of Geophysical Research 111*, D08203, doi: 10.1029/2005JD006586.

Dessler, A., S. Palm, and J. Spinhirne (2006), Tropical cloud-top height distributions revealed by the Ice, Cloud, and land Elevation Satellite (ICESat)/Geoscience Laser Altimeter System (GLAS), *Journal of Geophysical Research, 111*, D12215, doi:10.1029/2005JD006705.

Dolan, K., J. Masek, C. Huang, and G. Sun (2009), Regional forest growth measured by combining ICESat GLAS and Landsat data, *Journal of Geophysical Research*, *114*, G00E05, doi:10.1029/2008JG000893.

DongChen, E., Q. Shen, Y. Xu, and G. Chen (2009), High-accuracy topographical information extraction based on fusion of ASTER stereo-data and ICESat/GLAS data in Antarctica, *Science in China Series D-Earth Sciences*, *52* (5), 714-722.

Drews, R., W. Rack, C. Wesche, and V. Helm (2009), A spatially adjusted elevation model in Dronning Maud Land, Antarctica, based on differential SAR interferometry, *IEEE Transactions on Geoscience and Remote Sensing*, *47* (8), 2501-2509.

Duong, H., N. Pfeifer, and R. Lindenbergh (2006), Analysis of repeated ICESat full waveform data: Methodology and leaf-on/leaf-off comparison, *Proceedings of the Workshop on 3D Remote Sensing in Forestry*, 14-15 February, Vienna, Austria.

Duong, H., R. Lindenbergh, N. Pfeifer, and G. Vosselman (2007), Error analysis of ICESat waveform processing by investigating overlapping pairs over Europe, *IGARSS 2007: Proceedings of the IEEE International Geoscience and Remote Sensing Symposium*, 23-27 July, Barcelona, Spain, 4753-4756.

Duong, V., R. Lindenbergh, N. Pfeifer, and G. Vosselman (2008), Single and two epoch analysis of ICESat full waveform data over forested areas, *International Journal of Remote Sensing*, *29* (5), 1453-1473.

Eguchi, N., T. Yokota, and G. Inoue (2007), Characteristics of cirrus clouds from ICESat/GLAS observations, *Geophysical Research Letters*, 34, L09810, doi: 10.1029/2007GL029529.

Farrell, S. and S. Laxon (2004), Using ICESat/GLAS to detect changes in Arctic sea ice, *Proceedings of the 55th International Astronautical Congress*, 4-8 October, Vancouver, Canada, IAC-04-B.4.08.

Farrell, S., S. Laxon, D. McAdoo, D. Yi, and H. J. Zwally (2009), Five years of Arctic sea ice freeboard measurements from ICESat, *Journal of Geophysical Research*, *114*, C04008, doi:10.1029/2008JC005074.

Filin, S. (2006), Calibration of spaceborne laser altimeters - an algorithm and the site selection problem, *IEEE Transactions on Geoscience and Remote Sensing*, *44* (6), 1484-1492.

Forsberg, R. and H. Skourup (2005), Arctic Ocean gravity, geoid and sea-ice freeboard heights from ICESat and GRACE, *Geophysical Research Letters 32*, L21502, doi: 10.1029/2005GL023711.

Fowell, R., N. Smith, S. Bae, B. Schutz (2009), Bad stars, *Advances in the Astronautical Sciences*, *133*, 19-36.

Fricker, H., J. Bassis, J.-B. Minster, and D. MacAyeal (2005), ICESat's new perspective on ice shelf rifts: The vertical dimension, *Geophysical Research Letters*, 32, L23S08, doi:10.1029/2005GL025070.

Fricker, H., A. Borsa, J.-B. Minster, C. Carabajal, K. Quinn, and B. Bills (2005), Assessment of ICESat performance at the Salar de Uyuni, Bolivia, *Geophysical Research Letters*, *32*, L21S06, doi:10.1029/2005GL023423.

Fricker, H., N. Young, R. Coleman, J. Bassis, and J.-B. Minster (2005), Multi-year monitoring of rift propagation on the Amery Ice Shelf, East Antarctica, *Geophysical Research Letters, 32*, L02502, doi:10.1029/2004GL021036.

Fricker, H. and L. Padman (2006), Ice shelf grounding zone structure from ICESat laser altimetry, *Geophysical Research Letters*, 33, L15502, doi: 10.1029/2006GL026907.

Fricker, H., T. Scambos, R. Bindschadler, and L. Padman (2007), An active subglacial water system in West Antarctic mapped from space, *Science*, *315*, 1544-1548.

Fricker, H. and T. Scambos (2009), Connected subglacial lake activity on lower Mercer and Whillans ice streams, West Antarctica, 2003–2008, *Journal of Glaciology*, *55* (190), 303-315.

Fricker, H., R. Coleman, L. Padman, T. Scambos, J. Bohlander, and K. Brunt (2009), Mapping the grounding zone of the Amery Ice Shelf, East Antarctica using InSAR, MODIS and ICESat, *Antarctic Science*, *21* (5), 515-532, doi:10.1017/S095410200999023X.

Griggs, J. and J. Bamber (2009), A new 1 km digital elevation model of the Antarctic derived from combined satellite radar and laser data – Part 2: validation and error estimates, *The Cryosphere*, *3*, 113-123.

Grob, E., C. Baker, and T. McCarthy (2004), Geoscience Laser Altimeter System(GLAS) loop heat pipes: An eventful first year on-orbit, Paper 2004-01-2558, *34th International Conference on Environmental Systems*, Colorado Springs, Colorado, 19-22 July.

GSFC (2009), Plan for continued operation and additional scientific advances with the ICESat mission: exploring the Earth in three dimensions, NASA Senior Review, 24 March.

Gunter, B., T. Urban, R. Riva, M. Helsen, R. Harpold, S. Poole, P. Nagel, B. Schutz, and B. Tapley (2009), A comparison of coincident GRACE and ICESat data over Antarctica, *Journal of Geodesy*, *83* (11), 1051-1060.

Hakun, C., J. Budinoff, G. Brown, F. Parong, and A. Morell (2004), A boresight adjustment mechanism for use on laser altimeters, *Proceedings of the 37th Aerospace Mechanisms Symposium*, Houston, Texas, 19-21 May, 45-58.

Hanjiang, W. and C. Pengfei (2005), Introduction to principle of ICESat/GLAS laser altimetry and its applications, *Science of Surveying and Mapping*, *30* (5), 33-35.

Harding, D. and C. Carabajal (2005), ICESat waveform measurements of within-footprint topographic relief and vegetation vertical structure, *Geophysical Research Letters*, *32*, L21S10, doi:10.1029/2005GL023471.

Hart, W., J. Spinhirne, S. Palm, and J. Spinhirne (2005), GLAS spaceborne lidar observations of clouds and aerosols, *Óptica Pura y Aplicada*, *39* (1), 117-123.

Hart, W., J. Spinhirne, S. Palm, and D. Hlavka (2005), Height distribution between cloud and aerosol layers from the GLAS spaceborne lidar in the Indian Ocean region, *Geophysical Research Letters*, *32*, L22S06, doi:10.1029/2005GL023671.

Helmer, E. and M. Lefsky (2006), Forest canopy heights in Amazon River basin forests as estimated with the Geoscience Laser Altimeter System (GLAS), *USDA Forest Service Proceedings*, RMRS-P-42CD.

Helmer, E., M. Lefsky, and D. Roberts (2009), Biomass accumulation rates of Amazonian secondary forest and biomass of old-growth forests from Landsat time series and the Geoscience Laser Altimeter System, *Journal of Applied Remote Sensing*, *3* (1), 033505, doi:10.1117/1.3082116.

Herzfeld, U., P. McBride, H. Zwally, and J. DiMarzio (2008), Elevation changes in Pine Island Glacier, Walgreen Coast, Antarctica, based on GLAS (2003) and ERS-1 (1995) altimeter data analyses and glaciological implications, *International Journal of Remote Sensing*, *29* (19), 5533-5553.

Hese, S., W. Lucht, C. Schmullius, M. Barnsley, R. Dubayah, D. Knorr, K. Neumann, T. Riedel, and K. Schröter (2005), Global biomass mapping for an improved understanding of the CO2 balance — The Earth Observation mission Carbon-3D, *Remote Sensing of Environment*, *94* (1), 94-104.

Heyder, U. (2005), Vertical forest structure from ICESat/GLAS LIDAR data, M.Sc. Thesis, 118 pp., University College London, London, England.

Hlavka, D., S. Palm, W. Hart, J. Spinhirne, M. McGill, and E. Welton (2005), Aerosol and cloud optical depth from GLAS: Results and verification for an October 2003 California fire smoke case, *Geophysical Research Letters*, *32*, L22S07, doi: 10.1029/2005GL023413.

Hoff, R., S. Palm, J. Engel-Cox, and J. Spinhirne (2005), GLAS long-range transport observation of the 2003 California forest fire plumes to the northeastern US, *Geophysical Research Letters, 32*, L22S08, doi: 10.1029/2005GL023723.

Horgan, H. and S. Anandakrishnan (2006), Static grounding lines and dynamic ice streams: Evidence from the Siple Coast, West Antarctica, *Geophysical Research Letters*, *33*, L18502, doi: 10.1029/2006GL027091.

Howat, I., B. Smith, I. Joughin, and T. Scambos (2008), Rates of southeast Greenland ice volume loss from combined ICESat and ASTER observations, *Geophysical Research Letters*, *35*, L17505, doi: 10.1029/2008GL034496.

Hulbe, C., T. Scambos, T. Youngberg, and A. Lamb (2008), Patterns of glacier response to disintegration of the Larsen B ice shelf, Antarctic Peninsula, *Global and Planetary Change*, *63* (1), 1-8.

Jansen, D., M. Schodlok, and W. Rack (2007), Basal melting of A-38B: A physical model constrained by satellite observations, *Remote Sensing of Environment*, *111* (2-3), 195-203.

Joughin, I. and J. Bamber (2005), Thickening of the ice stream catchments feeding the Filchner-Ronne Ice Shelf, Antarctica, *Geophysical Research Letters*, *32*, L17503, doi: 10.1029/2005GL023844.

Joughin, I., J. Bamber, T. Scambos, S. Tulaczyk, M. Fahnestock, and D. MacAyeal (2006), Integrating satellite observations with modeling: basal shear stress of the Filcher-Ronne ice streams, Antarctica, *Philosophical Transactions of the Royal Society of London, Series A*, *364* (1844), 1795-1814.

Kaab, A. (2008), Glacier volume changes using ASTER satellite stereo and ICESat GLAS laser altimetry. A Test Study on EdgeØya, Eastern Svalbard, *IEEE Transactions on Geoscience and Remote Sensing Journal, 46* (10), 2823-2830.

King, M., R. Coleman, A.-J. Freemantle, H. Fricker, R. Hurd, B. Legrésy, L. Padman, and R. Warner, (2009), A 4-decade record of elevation change of the Amery Ice Shelf, East Antarctica, *Journal of Geophysical Research, 114*, C04004, doi:10.1029/2008JC005116.

Korona, J., E. Berthier, M. Bernard, F. Rémy, and E. Thouvenot (2009), SPIRIT. SPOT 5 stereoscopic survey of Polar Ice: Reference Images and Topographies during the fourth International Polar Year (2007-2009), *ISPRS Journal of Photogrammetry and Remote Sensing*, *64* (2), 204-212, doi:10.1016/j.isprsjprs.2008.10.005.

Kovacs, T. (2006), Comparing MODIS and AERONET aerosol optical depth at varying separation distances to assess ground-based validation strategies for spaceborne LIDAR, *Journal of Geophysical Research*, *111*, D24203, doi: 10.1029/2006JD007349.

Kurtz, N., T. Markus, D. Cavalieri, W. Krabill, J. Sonntag, and J. Miller (2008), Comparison of ICESat data with airborne laser altimeter measurements over Arctic sea ice, *IEEE Transactions on Geoscience and Remote Sensing*, *46* (7), 1913-1924.

Kwok, R., H. Zwally, and D. Yi (2004), ICESat observations of Arctic sea ice: A first look, *Geophysical Research Letters*, *31*, L16401, doi:10.1029/2004GL020309.

Kwok, R. and H. Zwally (2006), ICESat over Arctic sea ice: Interpretation of altimetric and reflectivity profiles, *Journal of Geophysical Research*, *111*, C06006, doi: 10.1029/2005JC003175.

Kwok, R., G. Cunningham, H. Zwally, and D. Yi (2007), Ice, Cloud, and land Elevation Satellite (ICESat) over Arctic sea ice: Retrieval of freeboard, *Journal of Geophysical Research*, *112*, C12013, doi: 10.1029/2006JC003978.

Kwok, R. and G. Cunningham (2008), ICESat over Arctic sea ice: Estimation of snow depth and ice thickness, *Journal of Geophysical Research*, *113*, C08010, doi: 10.1029/2008JC004753.

Kwok, R., G. Cunningham, M. Wensnahan, I. Rigor, H. Zwally, and D. Yi (2009), Thinning and volume loss of the Arctic Ocean sea ice cover: 2003-2008, *Journal of Geophysical Research*, *114*, C07005, doi:10.1029/2009JC005312.

Kwok, R. and D. Rothrock (2009), Decline in Arctic sea ice thickness from submarine and ICESat records: 1958-2008, *Geophysical Research Letters*, *36*, L15501, doi:10.1029/2009GL039035.

Lancaster, R., J. Spinhirne, and S. Palm (2005), Laser pulse reflectance of the ocean surface from the GLAS satellite lidar, *Geophysical Research Letters*, *32*, L22S10, doi: 10.1029/2005GL023732.

Lefsky, M., D. Harding, M. Keller, W. Cohen, C. Carabajal, F. del Bom Espirito-Santo, M. Hunter, and R. de Oliveira (2005), Estimates of forest canopy height and aboveground biomass using ICESat, *Geophysical Research Letters*, 32, L22S02, doi: 10.1029/2005GL023971.

Lefsky, M., M. Keller, Y. Panga, P. de Camargod, and M. Hunter (2007), Revised method for forest canopy height estimation from Geoscience Laser Altimeter System waveforms, *Journal of Applied Remote Sensing*, *1*, 013537.

Lefsky, M. (2010), A global forest canopy height map from the Moderate Imaging Spectroradiometer and the Geoscience Laser Altimeter System, *Geophysical Research Letters*, *37*, L15401, doi:10.1029/2010GL043622.

Liu, C. (2007), Geographical and seasonal distribution of tropical tropopause thin clouds and their relation to deep convection and water vapor viewed from satellite measurements, *Journal of Geophysical Research*, *112*, D09205, doi: 10.1029/2006JD007479.

Luthcke, S., D. Rowlands, T. Williams, and M. Sirota (2005), Reduction of ICESat systematic geolocation errors and the impact on ice sheet elevation change detection, *Geophysical Research Letters*, *32*, L21S05, doi:10.1029/ 2005GL023689.

Magruder, L., E. Silverberg, C. Webb, and B. Schutz (2005), In situ timing and pointing verification of the ICESat altimeter using a ground-based system, *Geophysical Research Letters, 32*, L21S04, doi:10.1029/2005GL023504.

Magruder, L., C. Webb, T. Urban, E. Silverberg, and B. Schutz (2007), ICESat altimetry data product verification at White Sands Space Harbor, *IEEE Transactions on Geoscience and Remote Sensing*, *45* (1), 147-155.

Mahesh, A., M. Gray, S. Palm, W. Hart, and J. Spinhirne (2004), Passive and active detection of clouds: Comparisons between MODIS and GLAS observations, *Geophysical Research Letters*, *31*, L04108, doi:10.1029/2003GL018859

Martin, C., R. Thomas, W. Krabill, and S. Manizade (2005), ICESat range and mounting bias estimation over precisely-surveyed terrain, *Geophysical Research Letters*, *32*, L21S07, doi:10.1029/2005GL023800.

McAdoo, D., S. Farrell, S. Laxon, H. Zwally, D. Yi, and A. Ridout (2008), Arctic Ocean gravity field derived from ICESat and ERS-2 altimetry: Tectonic implications, *Journal of Geophysical Research*, *113*, B05408, doi: 10.1029/2007JB005217.

Minnis, P., L. Nguyen, R. Palikonda, P. Heck, D. Spangenberg, D. Doelling, J. Ayers, W. Smith, M. Kaiyer, Q. Trepte, et al. (2008), Near-real time cloud retrievals from operational and research meteorological satellites, in *Remote Sensing of Clouds and the Atmosphere XIII*, *Proceedings of SPIE*, *Vol. 7107*, edited by R. Picard, A. Comeron, K. Schaufer, A. Amodeo, and M. van Weele, doi: 10.1117/12.800344.

Muskett, R., C. Lingle, J. Sauber, B. Rabus, and W. Tangborn (2008), Acceleration of surface lowering on the tidewater glaciers of Icy Bay, Alaska, USA from InSAR DEMs and ICESat altimetry, *Earth and Planetary Science Letters*, *265* (3-4), 345-359.

Muskett, R., C. Lingle, J. Sauber, A. Post, W. Tangborn, B. Rabus, and K. Echelmeyer (2009), Airborne and spaceborne DEM- and laser altimetry-derived surface elevation and volume changes of the Bering Glacier system, Alaska, USA, and Yukon, Canada, 1972–2006, *Journal of Glaciology*, *55* (190), 316-326.

Naud, C., J. Muller, and P. de Valk (2005), On the use of ICESat-GLAS measurements for MODIS and SEVIRI cloud-top height accuracy assessment, *Geophysical Research Letters*, *32*, L19815, doi:10.1029/2005GL023275.

Nelson, R., J. Boudreau, T. Gregoire, H. Margolis, E. Naesset, T. Gobakken, and G. Stahl (2009), Estimating Quebec provincial forest resources using ICESat/GLAS, *Canadian Journal of Forest Research*, *39* (4), 862-881.

Nelson, R., K. Ranson, G. Sun, D. Kimes, V. Kharuk, and P. Montesano (2009), Estimating Siberian timber volume using MODIS and ICESat/GLAS, *Remote Sensing of Environment*, *113* (3), 691-701.

Nerem, R., E. Leuliette, and A. Cazenave (2006), Present-day sea-level change: A review, *Comptes Rendus Geoscience*, *338* (14-15), 1077-1083.

Neuenschwander, A., T. Urban, R. Gutierrez, and B. Schutz (2008), Characterization of ICESat/GLAS waveforms over terrestrial ecosystems: Implications for vegetation mapping, *Journal of Geophysical Research*, *113*, G02S03, doi: 10.1029/2007JG000557.

Nguyen, A. and T. Herring (2005), Analysis of ICESat data using Kalman filter and kriging to study height changes in East Antarctica, *Geophysical Research Letters*, *32*, L23S03, doi:10.1029/2005GL024272.

Nuth, C., G. Moholdt, J. Kohler, J. O. Hagen, and A. Kääb (2010), Svalbard glacier elevation changes and contribution to sea level rise, *Journal of Geophysical Research*, *115*, F01008, doi:10.1029/2008JF001223.

Padman, L. and H. Fricker (2005), Tides on the Ross Ice Shelf observed with ICESat, *Geophysical Research Letters*, *32*, L14503, doi:10.1029/2005GL023214.

Padman, L., S. Erofeeva, and H. Fricker (2008), Improving Arctic tide models by assimilation of ICESat laser altimetry over ice shelves, *Geophysical Research Letters*, *35*, L22504, doi:10.1029/2008GL035592.

Palm, S., A. Benedetti, and J. Spinhirne (2005), Validation of ECMWF global forecast model parameters using the GLAS atmospheric channel measurements, *Geophysical Research Letters*, *32*, L22S09, doi:10.1029/2005GL023535.

Palm, S., M. Fromm, and J. Spinhirne (2005), Observations of Antarctic polar stratospheric clouds by the Geoscience Laser Altimeter System (GLAS), *Geophysical Research Letters*, *32*, L22S04, doi:10.1029/2005GL023524.

Plana-Fattori, A., G. Brogniez, P. Chervet, M. Haeffelin, O. Lado-Bordowsky, Y. Morille, F. Parol, J. Pelon, A. Roblin, G. Sèze, and C. Stubenrauch (2009), Comparison of high-cloud characteristics as estimated by selected spaceborne observations and ground-based lidar datasets, *Journal of Applied Meteorology and Climatology*, *48* (6), 1142-1160.

Potts, L., O. Akyilmaz, A. Braun, and C. Shum (2008), Multi-resolution dune morphology using Shuttle Radar Topography Mission (SRTM) and dune mobility from fuzzy inference systems using SRTM and altimetric data, *International Journal of Remote Sensing*, *29* (10), 2879–2901.

Pritchard, H., R. Arthern, D. Vaughan, and L. Edwards (2009), Extensive dynamic thinning on the margins of the Greenland and Antarctic ice sheets, *Nature*, *461*, 971-975, doi:10.1038/nature08471.

Ranson, K., G. Sun, K. Kovacs, and V. Kharuk (2004), Landcover attributes from ICESat GLAS data in central Siberia, *IGARSS 2004: Proceedings of the IEEE Geoscience and Remote Sensing Symposium,* Anchorage, Alaska, 20-24 September, 753-756.

Ranson, K., G. Sun, K. Kovacs, and V. Kharuk (2004), Use of ICESat GLAS data for forest disturbance studies in central Siberia, *IGARSS 2004: Proceedings of the IEEE Geoscience and Remote Sensing Symposium,* Anchorage, Alaska, 20-24 September, 1936-1939.

Ranson, K., R. Nelson, D. Kimes, D. Sun, V. Kharuk, and P. Montesano (2007), Using MODIS and GLAS data to develop timber volume estimates in central Siberia, *IGARSS 2007: Proceedings of the IEEE International Geoscience and Remote Sensing Symposium,* Barcelona, Spain, 23-27 July, 2306-2309.

Ray, R. (2008), A preliminary tidal analysis of ICESat laser altimetry: Southern Ross Ice Shelf, *Geophysical Research Letters*, 35, L02505, doi: 10.1029/2007GL032125.

Rignot, E., G. Casassa, S. Gogineni, P. Kanagaratnam, W. Krabill, H. Pritchard, A. Rivera, R. Thomas, J. Turner, and D. Vaughan (2005), Recent ice loss from the Fleming and other glaciers, Wordie Bay, West Antarctic Peninsula, *Geophysical Research Letters*, *32*, L07502, doi:10.1029/2004GL021947.

Rignot, E. (2006), Changes in ice dynamics and mass balance of the Antarctic ice sheet, *Philosophical Transactions of the Royal Society A: Mathematical, Physical and Engineering Sciences*, *364* (1844), 1637-1655.

Rim, H., C. Webb, S. Yoon, and B. Schutz (2007), Macro-model tuning experiment for ICESat precision orbit determination, *Advances in the Astronautical Sciences*, *127*, 987-996.

Roemer, S., B. Legrésy, M. Horwath, and R. Dietrich (2007), Refined analysis of radar altimetry data applied to the region of the subglacial Lake Vostok/Antarctica, *Remote Sensing of Environment*, *106* (3), 269-284.

Rosette, J., P. North, and J. Suárez (2008), Vegetation height estimates for a mixed temperate forest using satellite laser altimetry, *International Journal of Remote Sensing*, *29* (5), 1475-1493.

Rothrock, D., D. Percival, and M. Wensnahan (2008), The decline in Arctic sea-ice thickness: separating the spatial, annual, and interannual variability in a quarter-century of submarine data, *Journal of Geophysical Research*, *113*, C05003, doi:10.1029/2007JC004252.

Sauber, J., B. Molnia, C. Carabajal, S. Luthcke, and R. Muskett (2005), Ice elevations and surface change on the Malaspina Glacier, Alaska, *Geophysical Research Letters*, *32*, L23S01, doi:10.1029/2005GL023943.

Scambos, T., J. Bohlander, C. Shuman, and P. Skvarca (2004), Glacier acceleration and thinning after ice shelf collapse in the Larsen B Embayment, Antarctica, *Geophysical Research Letters*, *31*, L18402, doi:10.1029/ 2004GL020670.

Scambos, T., O. Sergienko, A. Sargent, D. MacAyeal, and J. Fastook (2005), ICESat profiles of tabular iceberg margins and iceberg breakup at low latitudes, *Geophysical Research Letters*, *32*, L23S09, doi:10.1029/2005GL023802.

Scambos, T., R. Ross, R. Bauer, Y. Yermolin, P. Skvarca, D. Long, J. Bohlander, T. Haran (2008), Calving and ice shelf break-up processes investigated by proxy: Antarctic tabular iceberg evolution during northward drift, *Journal of Glaciology 54* (187), 579-591, doi:10.3189/002214308786570836.

Schenk, T., B. Csatho, C. van der Veen, H. Brecher, Y. Ahn, and T. Yoon (2005), Registering imagery to ICESat data for measuring elevation changes on Byrd Glacier, Antarctica, *Geophysical Research Letters, 32*, L23S05, doi:10.1029/2005GL024328.

Schutz, B., H. Zwally, C. Shuman, D. Hancock, and J. DiMarzio (2005), Overview of the ICESat mission, *Geophysical Research Letters, 32*, L21S01, doi:10.1029/2005GL024009.

Schutz, B. (2005), Geolocation for the ICESat laser altimeter, *Advances in the Astronautical Sciences*, *121*, 127-142.

Scott, J., G. Gudmundsson, A. Smith, R. Bingham, H. Pritchard, and D. Vaughan (2009), Increased rate of acceleration on Pine Island Glacier strongly coupled to changes in gravitational driving stress, *The Cryosphere, 3*, 125-131.

Sèze, G., F. Parol, J. Pelon, C. Vanbauce, H. Legleau, M. Derrien, M. Lalande, and J. Buriez (2006), Comparison of SEVIRI cloud product with both the POLDER and the GLAS space Lidar one, *Proceedings of the 3rd MSG RAO Workshop* (ESA SP-619), 15 June, Helsinki, Finland, 37.

Sharov, A. and S. Etzold (2005), Upgrading interferometric models of European tidewater glaciers with altimetry data, *Proceedings of the CryoSat 2005 Workshop*, 8-10 March, Frascati, Italy.

Shiobara, M., M. Yabuki, R. Neuber, J. Spinhirne, E. Welton, J. Campbell, W. Hart, and T. Berkoff (2006), Arctic experiment for ICESat/GLAS ground validation with a micro-pulse LIDAR at Ny-Alesund, Svalbard, *Polar Meteorology and Glaciology*, *20*, 28–39.

Shuman, C., H. Zwally, B. Schutz, A. Brenner, J. DiMarzio, V. Suchedo, and H. Fricker (2006), ICESat Antarctic elevation data: Preliminary precision and accuracy assessment, *Geophysical Research Letters*, *33*, L07501, doi: 10.1029/2005GL025227.

Simard, M., V. Rivera-Monroy, J. Mancera-Pineda, E. Castañeda-Moya, and R. Twilley (2008), A systematic method for 3D mapping of mangrove forests based on Shuttle Radar Topography Mission elevation data, ICESat/GLAS waveforms and field data: Application to Ciénaga Grande de Santa Marta, Colombia, *Remote Sensing of Environment*, *112* (5), 2131-2144.

Sirota J., Millar P., C. Field, D. Mostofi, E. Ketchum, C. Carabajal, and S. Luthcke (2004), Laser pointing determination system for the Geoscience Laser Altimeter on ICESat: Initial in-flight performance assessment, *Advances in the Astronautical Sciences*, *118*, 607-622.

Sirota, J. M., S. Bae, P. Millar, D. Mostofi, C. Webb, B. Schutz, and S. Luthcke (2005), The transmitter pointing determination in the Geoscience Laser Altimeter System, *Geophysical Research Letters, 32*, L22S11, doi:10.1029/2005GL024005.

Skourup, H. and R. Forsberg (2008), Geoid, sea level and vertical datum of the Arctic - improved by ICESat and GRACE, *Geomatica*, *62*, 287-298.

Slobbe, D., R. Lindenbergh, and P. Ditmar (2008), Estimation of volume change rates of Greenland's ice sheet from ICESat data using overlapping footprints, *Remote Sensing of Environment*, *112* (12), 4204-4213.

Slobbe, D., P. Ditmar, and R. Lindenbergh (2009), Estimating the rates of mass change, ice volume change and snow volume change in Greenland from ICESat and GRACE data, *Geophysical Journal International*, *176* (1), 95-106.

Smith, B., C. Bentley, and C. Raymond (2005), Recent elevation changes on the ice streams and ridges of the Ross Embayment from ICESat crossovers. *Geophysical Research Letters*, 32, L21S09, doi: 10.1029/2005GL024365.

Smith, B., H. Fricker, I. Joughin, and S. Tulaczyk (2009), An inventory of active subglacial lakes in Antarctica detected by ICESat (2003-2008), *Journal of Glaciology*, *55* (192), 573-595.

Spinhirne, J., S. Palm, and W. Hart (2005), Antarctica cloud cover for October 2003 from GLAS satellite lidar profiling, *Geophysical Research Letters, 32*, L22S05, doi:10.1029/2005GL023782.

Spinhirne, J., S. Palm, W. Hart, D. Hlavka, and E. Welton (2005), Cloud and aerosol measurements from GLAS: Overview and initial results, *Geophysical Research Letters*, *32*, L22S03, doi:10.1029/2005GL023507.

Spinhirne, J., S. Palm, D. Hlavka, W. Hart, and E. Welton (2005), Global aerosol distribution from the GLAS polar orbiting lidar instrument, *IEEE Workshop on Remote Sensing of Atmospheric Aerosols*, 5-6 April, Tucson, Arizona, 2-8.

Spinhirne, J. (2008), Performance of the GLAS satellite LIDAR cloud and aerosol measurements, *Proceedings of the IEEE Aerospace Conference 2008*, 1-8, doi:10.1109/aero.2008.4526389.

Spreen, G., S. Kern, D. Stammer, R. Forsberg, and J. Haartpaintner (2006), Satellite-based estimates of sea-ice volume flux through Fram Strait, *Annals of Glaciology*, *44* (1), 321-328.

Spreen, G., S. Kern, D. Stammer, and E. Hansen (2009), Fram Strait sea ice volume export estimated between 2003 and 2008 from satellite data, *Geophysical Research Letters*, *36*, L19502, doi:10.1029/2009GL039591.

Sun, G., K. Ranson, D. Kimes, J. Blair, and K. Kovacs (2008), Forest vertical structure from GLAS: An evaluation using LVIS and SRTM data, *Remote Sensing of Environment*, *112* (1), 107-117.

Surazakov, A. and V. Aizen (2006), Estimating volume change of mountain glaciers using SRTM and map-based topographic data, *IEEE Transactions on Geoscience and Remote Sensing*, *44* (10), 2991-2995.

Thomas, R., E. Rignot, G. Casassa, P. Kanagaratnam, C. Acuña, T. Atkins, H. Brecher, E. Frederick, P. Gogineni, W. Krabill, et al. (2004), Accelerated sea-level rise from West Antarctica, *Science*, *306* (5694), 255-258.

Thomas, R., E. Frederick, W. Krabill, S. Manizade, C. Martin, and A. Mason (2005), Elevation changes on the Greenland Ice Sheet from comparison of aircraft and ICESat laser-altimeter data, *Annals of Glaciology*, *42* (1), 77-82.

Urban, T., B. Schutz, and A. Neuenschwander (2008), A survey of ICESat coastal altimetry applications: Continental coast, open ocean island, and inland river, *Terrestrial Atmospheric and Oceanic Sciences Journal*, *19* (1-2), 1-19.

Urban, T. and B. Schutz (2005), ICESat sea level comparisons, *Geophysical Research Letters*, *32*, L23S10, doi:10.1029/2005GL024306.

Van den Broeke, M., W. van de Berg, and E. van Meijgaard (2008), Firn depth correction along the Antarctic grounding line, *Antarctic Science*, *20*, 513-517.

Wang, L. and A. Dessler (2006), Instantaneous cloud overlap statistics in the tropical area revealed by ICESat/GLAS data, *Geophysical Research Letters*, *33*, L15804, doi:10.1029/2005GL024350.

Wang, X., M. Frontoso, G. Pisani, and N. Spinelli (2007), Retrieval of atmospheric particles optical properties by combining ground-based and spaceborne lidar elastic scattering profiles, *Optics Express*, *15* (11), 6734-6743.

Webb, C., J. Stauch, R. Harpold, K. Lorhammer, B. Schutz, and G. Born (2005), ICESat off-nadir laser targeting: Theory and practice, *Advances in the Astronautical Sciences*, *123*, 155-174.

Webb, C. (2007), Radiation Force Modeling for ICESat precision orbit determination, Ph.D. dissertation, 311 pp., University of Texas at Austin, Austin, Texas.

Webb, C., S. Bae, and B. Schutz (2010), Laser targeting performance in the ICESat mission, Abstract C41A-0486, AGU Fall Meeting, San Francisco, California, 13-17 December.

Wen, J., K. Jezek, B. Csathó, U. Herzfeld, K. Farness, and P. Huybrechts (2007), Mass budgets of the Lambert, Mellor and Fisher glaciers and basal fluxes beneath their flowbands on Amery Ice Shelf, *Science in China Series D: Earth Sciences*, *50* (11), 1693-1706.

Wesche, C., O. Eisen, H. Oerter, D. Schulte, and D. Steinhage (2007), Surface topography and ice flow in the vicinity of the EDML deep-drilling site, Antarctica, *Journal of Glaciology*, *53* (182), 442-448.

Wesche, C., S. Riedel, and D. Steinhage (2009), Precise surface topography of the grounded ice ridges at the Ekströmisen, Antarctica, based on several geophysical data sets, *ISPRS Journal of Photogrammetry and Remote Sensing*, *64* (4), 381-386.

Wilkinson, J., R. Hogan, A. Illingworth, and A. Benedetti (2008), Use of a LIDAR forward model for global comparisons of cloud fraction between the ICESat LIDAR and the ECMWF Model, *Monthly Weather Review*, *136* (10), 3742–3759.

Winther, J.-G., R. Bindschadler, M. Konig, and D. Scherer (2005), Remote sensing of glaciers and ice sheets, *Geophysical Monograph*, *163*, 39-62.

Wu, W., A. Dessler, and G. North (2006), Analysis of the correlations between atmospheric boundary-layer and free-tropospheric temperatures in the tropics, *Geophysical Research Letters*, *33*, L20707, doi: 10.1029/2006GL026708.

Wylie, D., E. Eloranta, J. Spinhirne, and S. Palm (2007), A comparison of cloud cover statistics from the GLAS LIDAR with HIRS, *Journal of Climate*, *20* (19), 4968-4981.

Yamanokuchi, T., K. Doi, and K. Shibuya (2007), Combined use of InSAR and ICESat/GLAS data for high accuracy DEM generation on Antarctica, *IGARSS 2007: Proceedings of the IEEE International Symposium on Geoscience and Remote Sensing*, 23-27 July, Barcelona, Spain, 1229-1231.

Yi, D., H. Zwally, and X. Sun (2005), ICESat measurement of Greenland ice sheet surface slope and roughness, *Annals of Glaciology*, *42* (1), 83-89.

Yong, P., Y. Xinfang, L. Zengyuan, S. Guoqing, C. Erxue, and T. Bingxiang (2006), Waveform length extraction from ICESat GLAS data and forest application analysis, *Scientia Silvae Sinicae*, *42* (7), 137-140.

Zhang, X. and R. Forsberg (2007), Assessment of long-range kinematic GPS positioning errors by comparison with airborne laser altimetry and satellite altimetry, *Journal of Geodesy*, *81* (3), 201-211.

Zwally, H., B. Schutz, W. Abdalati, J. Abshire, C. Bentley, A. Brenner, J. Bufton, J. Dezio, D. Hancock, D. Harding, T. Herring, B. Minster, et al. (2002), ICESat's laser measurements of polar ice, atmosphere, ocean, and land, *Journal of Geodynamics*, *34*, 404-445.

Zwally, H., M. Giovinetto, J. Li, H. Cornejo, M. Beckley, A. Brenner, J. Saba, and D. Yi (2005), Mass changes of the Greenland and Antarctic ice sheets and shelves and contributions to sea-level rise: 1992-2002, *Journal of Glaciology*, *51* (175), 509-527.

Zwally, H., D. Yi, R. Kwok, and Y. Zhao (2008), ICESat measurements of sea ice freeboard and estimates of sea ice thickness in the Weddell Sea, *Journal of Geophysical Research*, *113*, C02S15, doi: 10.1029/2007JC004284.

Appendix A

Ice, Clouds and land Elevation Satellite (ICESat)
Mission Success Criteria
November 2002

National Aeronautics and Space Administration
Office of Earth Science

Ghassem R. Asrar

Associate Administrator for
Earth Science

Date

BACKGROUND

The Ice, Ground and land Elevation Satellite (ICESat) mission provides a subset of the overall Earth Observing System (EOS) program, primarily land and sea ice products. ICESat is planned to start a three year mission with a five year goal with a launch in December 2002.

ICESat MISSION OVERVIEW

The ICESat mission will measure changes in elevation of the Greenland and Antarctic ice sheets as part of NASA's Earth Observing System (EOS) of satellites. Time series of elevation changes will enable determination of the present day mass balance of the ice sheets, study of associations between observed ice changes and polar climate, and estimation of the present and future contributions of the ice sheets to the global sea level rise. Other scientific objectives of the ICESat include: global measurements of cloud heights and the vertical structure of clouds and aerosols; precise measurement of land topography and vegetation canopy heights; and measurements of sea ice roughness, sea ice thickness, ocean surface elevations, and surface reflectivity. The Geoscience Laser Altimeter System (GLAS) on the ICESat has a 1064 nm laser channel for surface altimetry and dense cloud heights and a 532 nm lidar channel for the vertical distribution of clouds and aerosols.

The ICESat will be launched into a 94° inclination, 600 km circular orbit with a 183 day repeat pattern. The on-board GPS receiver is designed to provide radial orbit determinations to better than 5 cm, and star trackers on board are designed to enable laser spot imaging footprints to 6 m horizontally. The spacecraft attitude control system should control the pointing of the laser beam to within ±35 m of reference surface tracks at high latitudes.

MISSION SUCCESS CRITERIA

Success for the ICESat mission is defined as an improvement by a significant factor over our current best knowledge, provided by radar altimetry, of the land ice elevation variability. Specifically:

1. Produce an improvement in the measurement of the land ice thickness variability over previous radar altimetry to $\delta(dh/dt) < 2$ cm/year (1σ value).
2. Produce calibrated profiles of global land and ocean surface elevations, especially at high latitudes where there is currently no detailed comprehensive data.
3. Produce calibrated profiles of ice sheet surface elevation to 25 cm accuracy at each laser illumination shot.